



This discussion paper is/has been under review for the journal *Climate of the Past* (CP).
Please refer to the corresponding final paper in CP if available.

NGRIP temperature reconstruction from 10 to 120 kyr b2k

P. Kindler¹, M. Guillevic^{2,3}, M. Baumgartner¹, J. Schwander¹, A. Landais², and M. Leuenberger¹

¹Climate and Environmental Physics, Physics Institute and Oeschger Centre for Climate Research, University of Bern, Bern, Switzerland

²Institut Pierre-Simon Laplace/Laboratoire des Sciences du Climat et de l'Environnement, Gif-sur-Yvette, France

³Centre for Ice and Climate, Niels Bohr Institute, University of Copenhagen, Copenhagen, Denmark

Received: 24 June 2013 – Accepted: 12 July 2013 – Published: 22 July 2013

Correspondence to: P. Kindler (kindler@climate.unibe.ch)

Published by Copernicus Publications on behalf of the European Geosciences Union.

CPD

9, 4099–4143, 2013

NGRIP temperature
reconstruction from
10 to 120 kyr b2k

P. Kindler et al.

Title Page

Abstract

Introduction

Conclusions

References

Tables

Figures



Back

Close

Full Screen / Esc

Printer-friendly Version

Interactive Discussion



Abstract

In order to reconstruct Greenland NGRIP temperature, measurements of $\delta^{15}\text{N}$ from the beginning of the Holocene to Dansgaard–Oeschger (DO) event 8 have been performed. Together with previously measured and mostly published $\delta^{15}\text{N}$ data, we are now able to present for the first time a NGRIP temperature reconstruction for the whole last glacial period (beginning of the Holocene back to 120 kyr) including every DO event based on $\delta^{15}\text{N}$ isotope measurements using a firn densification and heat diffusion model. The detected temperature rises at DO events range from 5 °C (DO 25) up to 16.5 °C (DO 11), ± 3 °C. To bring measured and modelled data into agreement, we had to reduce the accumulation rate given by the ss09sea06bm time scale in some periods significantly, especially during the last glacial maximum (LGM). A comparison between reconstructed temperature and $\delta^{18}\text{O}_{\text{ice}}$ data confirms that the isotopic composition of the stadial was strongly influenced by seasonality. We continuously calculated α ($\delta^{18}\text{O}_{\text{ice}}$ to temperature sensitivity) on a 10 kyr running time window. α variations show an anticorrelation with obliquity, in agreement with a simple Rayleigh distillation model, and moreover seem to be influenced by Northern Hemisphere ice sheet volume.

1 Introduction

First deep ice core drillings in Greenland revealed significant variability in the water isotopic composition $\delta^{18}\text{O}_{\text{ice}}$ during the last glacial compared to the relatively smooth Holocene (Johnsen et al., 1972; Dansgaard et al., 1982). When several deep ice cores have been drilled, all of which featured the same variability, it became obvious that these signals were of climatic origin (Johnsen et al., 1992; Dansgaard et al., 1982). Today these millennial time scale temperature instabilities are known as Dansgaard–Oeschger (DO) events and can be observed during the entire last glacial period.

NGRIP temperature reconstruction from 10 to 120 kyr b2k

P. Kindler et al.

Title Page

Abstract

Introduction

Conclusions

References

Tables

Figures

⏪

⏩

◀

▶

Back

Close

Full Screen / Esc

Printer-friendly Version

Interactive Discussion



NGRIP temperature reconstruction from 10 to 120 kyr b2k

P. Kindler et al.

Title Page

Abstract

Introduction

Conclusions

References

Tables

Figures



Back

Close

Full Screen / Esc

Printer-friendly Version

Interactive Discussion



The 25 DO events identified in the North Greenland Ice Core Project (NGRIP) ice core (NGRIP members, 2004) are characterised by a rapid temperature increase between 3 and 16°C within decades (Capron et al., 2012; Huber et al., 2006b; Landais et al., 2005; Lang et al., 1999; Severinghaus et al., 1998) followed by a gradual cooling back to stadial conditions. These rapid temperature variations are generally of northern hemispheric extent and can be traced in different climate proxies in ice cores, like $\delta^{18}\text{O}_{\text{ice}}$ (Dansgaard et al., 1993), dust content (Ruth et al., 2003) and other aerosol contents (Mayewski et al., 1997), greenhouse gas concentrations (Huber et al., 2006b; Schilt et al., 2010), as well as in other climate proxies such as sea sediments (Bond et al., 1993; Deplazes et al., 2013), lake sediments and speleothems (Fleitmann et al., 2009; Kanner et al., 2012; Wang et al., 2001).

It is widely assumed, that DO events are linked to reorganisations and/or variations in the strength of the Atlantic Meridional Overturning Circulation (AMOC) which transports heat from the equator to high northern latitudes. Different interactions between the AMOC and the stadial-interstadial-successions have been proposed. Some first concepts are mentioned in Broecker et al. (1985) where it is suggested that during stadials the AMOC and hence the deep-water formation is in a weak mode or even reversed whereas during DO events, the AMOC is in a strong mode condition. Another hypothesis is mentioned in Broecker et al. (1990) where a “salt oscillator” weakens and strengthens the AMOC. During an interstadial the salinity of the north Atlantic would decrease due to freshwater input of melting ice to a point where the newly produced deep water is not capable of flowing back into the southern ocean anymore. Consequently the AMOC would weaken and the climate shifts in a stadial where the salinity of the sea water would gradually increase based on the loss of water by evaporation and the reduced freshwater input until the seawater becomes dense enough to initiate the AMOC again. In Rahmstorf (2002) the idea of three different modes of ocean circulation is mentioned. In the “interstadial mode”, deep water is produced in the Nordic sea whereas in the “stadial mode” the AMOC is still in operation but the water sinks down to the deep ocean south of the shallow sill between Greenland and Scotland. In the

NGRIP temperature reconstruction from 10 to 120 kyr b2k

P. Kindler et al.

Title Page

Abstract

Introduction

Conclusions

References

Tables

Figures



Back

Close

Full Screen / Esc

Printer-friendly Version

Interactive Discussion



third “Heinrich mode” deep water formation ceases and deep water from the Antarctic region expands up to 62° N (Elliot et al., 2002). This sort of stadial is accompanied by a Heinrich (H) event, a massive discharge of icebergs from the Laurentide ice sheet into the Atlantic Ocean (Bond et al., 1993; Heinrich, 1988). Another suggestion is presented in Rasmussen and Thomsen (2004) where during stadial condition a halocline, caused by a layer of low saline, cold surface water, would prevent the formation of deep water. Due to the absence of outflow out of the Nordic sea, warmer North Atlantic water could have penetrated underneath the light surface water destabilising the halocline. By its breakdown warm deep water would rise to the surface triggering an onset of a DO event and re-establishing the AMOC. After a short period the formation of a melt water-lid would bring back the climate to stadial conditions.

The actual trigger for DO events remains unclear. Apart from these potential explanations mentioned above there is a hypothesis of a “stochastic resonance” (Alley et al., 2001). It is based on the fact that the DO events exhibit a spectral power of about 1500 yr and this together with noise in the context with ice sheets could lead to the observed patterns. In contrast, Ditlevsen et al. (2007) challenge the concept of a 1500 yr period, according to their statistical tests the periodicity strongly relies on the used time scale and can in some cases not been distinguished from a random occurrence. Another idea is that the DO events could have been triggered by solar forcing (Braun et al., 2005; Woillez et al., 2012) together with a combination of random variability (Braun and Kurths, 2010).

Recent research concerning the mechanisms of DO events points to a connection with sea ice (Li et al., 2010) where the rapid retreat and regrowth is able to alter Greenland’s temperature on decadal time scale or even shorter. Petersen et al. (2013) hypothesise that in stadials an extensive ice shelf east of Greenland together with sea ice in the Nordic Seas is responsible for cold Greenland temperatures. A subsequent ice shelf collapse probably due to subsurface water warming and a concomitant sea ice decrease would cause the rapid temperature increase at the onset of a DO event. In the following, the increased accumulation rates of the warmer climate would help

the ice shelf to regrow again which would lead to a gradual cooling until a threshold is attained where the sea ice is capable of restoring itself rapidly, leading finally to an accelerated cooling which shifts climate back to stadial conditions.

As Antarctic ice cores have shown, most of the DO events have an Antarctic analogue called Antarctic Isotope Maximum (AIM) (EPICA community members, 2006; Blunier and Brook, 2001; Capron et al., 2010a,b; Wolff et al., 2010). The slow AIM temperature increases precede the rapid Greenland warmings by several hundreds to thousands of years (Capron et al., 2010b) and are with a temperature amplitude of +1 to +3°C (Capron et al., 2010a; Stenni et al., 2010) far less pronounced than Greenland's DO events. The maximum warming in both hemispheres occur however contemporaneously (Capron et al., 2010b). A linear relationship between the duration of the Greenland stadial and the correspondent AIM warming amplitude was found for most of the DO events and AIM respectively (EPICA community members, 2006; Capron et al., 2010a). Exceptions are AIM 2 and 18 where this coherence does not apply, probably because of the extraordinary long duration of the Greenland stadials (Capron et al., 2010a; Vallelonga et al., 2012). These findings are in line with the concept of the "thermal bipolar seesaw" where the Southern Ocean is considered as a heat reservoir which delivers heat via the Atlantic Meridional Overturning Circulation to the North Atlantic and the Northern Sea (Stocker and Johnsen, 2003).

Another mechanism to link Greenland climate variability to climate alterations in regions around the equator is the southward shift of the Intertropical Convergence Zone (ITCZ) during Greenland cold (stadials and H) events (Chiang and Bitz, 2005). This southward shift of the ITCZ leads in the Northern Hemisphere to a drier East Asian (Wang et al., 2001) and Indian summer monsoon (Burns et al., 2003) and in the Southern Hemisphere to an intensified South American summer monsoon (Kanner et al., 2012).

Today, one distinguishes 25 DO events in the NGRIP ice core but it is not clear if the earliest one, DO 25, with its weak amplitude is an event like the subsequent ones or if it is simply a climate response to the gradual temperature decrease from

CPD

9, 4099–4143, 2013

NGRIP temperature reconstruction from 10 to 120 kyr b2k

P. Kindler et al.

Title Page

Abstract

Introduction

Conclusions

References

Tables

Figures



Back

Close

Full Screen / Esc

Printer-friendly Version

Interactive Discussion



NGRIP temperature reconstruction from 10 to 120 kyr b2k

P. Kindler et al.

Title Page

Abstract

Introduction

Conclusions

References

Tables

Figures



Back

Close

Full Screen / Esc

Printer-friendly Version

Interactive Discussion



the last interglacial to glacial conditions (Capron et al., 2012). Apart from the classical stadial-interstadial-pattern observed during the last glacial, Capron et al. (2010a) distinguished three kinds of sub-millennial scale variations in NGRIP ice based on the $\delta^{18}\text{O}_{\text{ice}}$ data: “precursor-type events” prior to the onset of an interstadial (e.g. DO 14, 21 and 23), “rebound-type events” with an abrupt increase at the end of the regular cooling phase (e.g. DO 12, 16 or even DO 23 with DO 22 as the corresponding rebound) and centennial-scale “abrupt coolings” during DO event 24.

The exact processes during DO climate variations are still not fully understood. Improved proxy climate records of the events will help to constrain possible mechanisms. The aim of this paper is to complete the temperature reconstruction over all Dansgaard–Oeschger events at the NGRIP site (NGRIP members, 2004). For the first time we present $\delta^{15}\text{N}$ data for the DO events 1 to 8. Previous work was performed by Huber et al. (2006b) (DO 9 to 17), Landais et al. (2004a, 2005) (DO 18 to 20, 23 and 24) and Capron et al. (2010a, 2012) (DO 21, 22 and 25). The combined records are used to establish a Greenland temperature record over a full glacial-interglacial cycle, namely from 10 to 120 kyr. We then investigate the sensitivity of water isotopes to temperature changes at millennial and orbital time scales.

2 Method

To reconstruct the surface temperature evolution at the NGRIP site we have used an approach consisting of $\delta^{15}\text{N}$ isotopic air measurements from ice cores (Severinghaus et al., 1998) together with a firn densification and heat diffusion model (Leuenberger et al., 1999; Lang et al., 1999; Huber et al., 2006b; Schwander et al., 1997).

The upper most 50 to 100 m of an ice sheet, where open pores dominate, which can still exchange air with the atmosphere, are called firn. In this layer the snow is gradually transformed to ice and at its bottom, at the lock-in depth (LID), air is enclosed into bubbles. The processes relevant for the results presented here occur in the firn. With respect to the air molecule mobility, one can divide the firn into three parts: convective,

diffusive and non-diffusive zones. In the generally small upper convective zone the composition of the air remains nearly unchanged compared to ambient air whereas one finds an enrichment in heavy molecules at the lower end of the diffusive zone due to gravitation, i.e. $^{15}\text{N}/^{14}\text{N}$ ratio is enhanced. With the barometric formula (Craig et al., 1988; Schwander, 1989) one finds (in delta-notation):

$$\delta^{15}\text{N}_{\text{grav}}(z) = \left(e^{\frac{\Delta m g z}{R T}} - 1 \right) \cdot 1000 \approx \frac{\Delta m \cdot g \cdot z}{R \cdot T} \cdot 1000 \quad (1)$$

where z is the depth of the diffusive zone, g the acceleration constant, Δm the mass difference between the isotopes, R the ideal gas constant and T the mean firn temperature. Present-day $\delta^{15}\text{N}$ measurements in firns show that no further gravitational enrichment occurs below the LID. A temperature gradient in the firn, e.g. established by a sudden warming at the snow surface, causes a second important process called thermal diffusion. Because gas diffuses about ten times faster than heat (Paterson, 1994) through the firn, this effect leads to an additional enrichment of the $^{15}\text{N}/^{14}\text{N}$ ratio at the bottom of the firn. Thermal diffusion can be characterised as (Severinghaus et al., 1998):

$$\delta^{15}\text{N}_{\text{therm}} = \left[\left(\frac{T_t}{T_b} \right)^{\alpha_T} - 1 \right] \cdot 1000 \approx \Omega \cdot \Delta T \quad (2)$$

where T_t and T_b stand for the temperature at the top and the bottom of the firn, α_T for the thermal diffusion constant ($\alpha_T = 4.61198 \times 10^{-3} \cdot \ln(\bar{T}/113.65\text{K})$, \bar{T} stands for the average firn temperature, Leuenberger et al., 1999), Ω for the thermal diffusion sensitivity and ΔT for the temperature difference ($T_t - T_b$). After several hundreds of years, when the temperature distribution in the firn is uniform again, the thermal diffusion effect disappears but the signal of rapid warming is preserved by the $^{15}\text{N}/^{14}\text{N}$ ratio in air enclosed in bubbles.

NGRIP temperature reconstruction from 10 to 120 kyr b2k

P. Kindler et al.

Title Page

Abstract

Introduction

Conclusions

References

Tables

Figures



Back

Close

Full Screen / Esc

Printer-friendly Version

Interactive Discussion



2.1 Data

The $\delta^{15}\text{N}$ data used for this work is a composite of measurements of two laboratories, Laboratoire des Sciences du Climat et de l'Environnement (LSCE), Gif-sur-Yvette (DO 18 to 25) and the Climate and Environmental Physics Division of the Physics Institute of the University of Bern (Holocene to DO 17). The data from Bern have been measured with an online setup (Huber et al., 2003; Huber and Leuenberger, 2004) where an up to 50 cm long ice sample is melted continuously on a melting device. The produced water-air-mixture is permanently pumped through a membrane to degas the water and the gaseous phase is analysed for its isotopic composition in a mass spectrometer. The data is corrected for the background, the chemical slope, the signal intensity imbalance effect and a drift in the mass spectrometer during a measurement (Huber and Leuenberger, 2004). The latter two corrections are obtained by measuring standard gas before and after the sample. The $\delta^{15}\text{N}$ data from the Holocene to DO 8 are published here for the first time whereas the data from DO 9 to DO 17 have been published in Huber et al. (2006b). 384 bags have been measured for the new data, 11 of them have been rejected due to a failure of the membrane. The remaining 373 bags have been divided into 600 data points, each representing 10 to 25 cm of ice (depending on the original sample length which is influenced by the ice availability and ice quality) with an uncertainty of $\pm 0.02\text{‰}$ in $\delta^{15}\text{N}$ (Huber and Leuenberger, 2004). The ice-samples which have been investigated at LSCE have been measured with a melt-refreeze technique and the extracted air was measured by a dual inlet mass spectrometer with a precision of $\pm 0.006\text{‰}$ in $\delta^{15}\text{N}$ (Landais et al., 2003, 2004c). Most of the $\delta^{15}\text{N}$ data over the period from DO 19 to DO 25 have been published: DO 18 to 20 in Landais et al. (2004a), DO 21 in Capron et al. (2010b), DO 22 in Capron et al. (2010a), DO 23 and 24 in Landais et al. (2005) and DO 25 in Capron et al. (2012). 41 data points between DO 20 and DO 21 and between DO 21 and 22 which were measured at LSCE are published here for the first time.

Title Page

Abstract

Introduction

Conclusions

References

Tables

Figures



Back

Close

Full Screen / Esc

Printer-friendly Version

Interactive Discussion



2.2 Temperature reconstruction

The temperature reconstruction was done with the firn densification and heat diffusion model from Schwander et al. (1997) by using the ss09sea06bm age scale (in years before 2000 AD or yr b2k) (NGRIP members, 2004; Johnsen et al., 2001) with some minor adjustments in the deepest part (Andersen et al., 2006). The ss09sea06bm age scale was chosen because it was the only time scale with also accumulation rates reconstructed over the entire time period. When one transfers our final model input to the GICC05 age scale, it leads only to minor changes in the model output compared to the used ss09sea06bm age scale, so we are confident that our results are valid for both age scales.

The input parameters of the model are age, accumulation rate and temperature. The temperature is calculated according to

$$T = (\delta^{18}\text{O}_{\text{ice}} + 35.1[\text{‰}]) / \alpha + 241.6 \text{ K} + \beta \quad (3)$$

where 35.1 ‰ and 241.6 K stand for NGRIP Holocene values (NGRIP members, 2004) and β for a temperature shift. The used accumulation and $\delta^{18}\text{O}_{\text{ice}}$ data from the ss09sea06bm time scale has been splined with a cut-off-period (COP) of 200 yr in order to reduce variability in the model output. The basic idea is to vary the temperature (α and β) and the accumulation rate in such a way that the model is able to reproduce the measured $\delta^{15}\text{N}$ data. The temperature reconstruction is divided into three steps: (i) rough adjustment of the temperature- $\delta^{18}\text{O}_{\text{ice}}$ -sensitivity (α) to approximate the shape of the modelled $\delta^{15}\text{N}$, (ii) refinement of the adjustment by varying the accumulation rate and a temperature shift for best fitting the Δage and (iii) final manual tuning where needed. The effect of each step on the modelled $\delta^{15}\text{N}$ and Δage can be seen for the time period DO 4 to 7 in Fig. 1.

In the first step, 19 different α -scenarios have been calculated by varying the α -value in 0.02 steps from 0.24 to 0.60 ‰ °C⁻¹. As in Huber et al. (2006b) the initial accumulation rate was reduced by 20 % and a constant temperature shift of $\beta = +4\text{K}$ was

CPD

9, 4099–4143, 2013

NGRIP temperature reconstruction from 10 to 120 kyr b2k

P. Kindler et al.

Title Page

Abstract

Introduction

Conclusions

References

Tables

Figures

⏪

⏩

◀

▶

Back

Close

Full Screen / Esc

Printer-friendly Version

Interactive Discussion



NGRIP temperature reconstruction from 10 to 120 kyr b2k

P. Kindler et al.

[Title Page](#)[Abstract](#)[Introduction](#)[Conclusions](#)[References](#)[Tables](#)[Figures](#)[Back](#)[Close](#)[Full Screen / Esc](#)[Printer-friendly Version](#)[Interactive Discussion](#)

introduced to match approximately the measured Δage . Without these corrections the modelled Δage is significantly underestimated in some parts, especially in the time period from 60 to 10 kyr. In order to find the best α in a 2 kyr time window, the sum of the squared differences between the $\delta^{15}\text{N}$ model-output of a scenario and the spline through the measured data was calculated and the scenario with the smallest sum was determined. Thereafter the time window was shifted continuously by 250 yr and the same procedure was applied until all data points were covered. At the end of step one, we obtain a “best” α -value every 250 yr, these values are splined for further calculations with a COP of 2 kyr. With these values, which vary roughly between 0.28 and 0.42 ‰°C⁻¹, the model is able to reproduce coarsely the measured $\delta^{15}\text{N}$ data (Fig. 1, blue lines).

To further refine the adjustment in a second step, the accumulation rate is varied from 60 to 100 % in 5 % steps and the temperature offset β from +0 to +8 K in 1 K steps while retaining the α -values from step one. This yields 81 different combinations and we proceed in the same way as in step one to find the best accumulation rate and temperature shift to match the measured $\delta^{15}\text{N}$ data. The adjusted accumulation rate varies roughly from 70 to 80 % for 12 to 64 kyr, from 90 to 100 % for 64 to 92 kyr and from 80 to 100 % for 92 to 123 kyr. The time dependent temperature shift β varies within 2 K around +4 K. With these three tuned parameters (α , β and accumulation) the model is able to reproduce the measured $\delta^{15}\text{N}$ data generally well, both the amplitudes as well as the timing of the DO events. The Δage output of the model and the calculated Δdepth are also in agreement with the measured data (Fig. 1, green lines).

The parts of the reconstruction which do not yet match are now tuned manually (on parameters β and accumulation) on short periods (centuries) in a third step so that the model is able to reproduce the measured data within their uncertainty (Fig. 1, red lines). A mismatch still exists in the Bølling Allerød-Younger Dryas-transition and in the periods of DO 16 and 17, DO 19 and 20 and DO 23 to 25. The tuning was done by adjusting the temperature evolution of a DO event or a certain time period between two fixed points in a linear way, e.g. the evolution of the temperature over a DO event was

increased or decreased between the onset and the end of the event. In addition, the accumulation rate was enhanced or lowered slightly in these parts where the timing was not yet satisfactory. After step three, modelled $\delta^{15}\text{N}$ as well as Δage and Δdepth are in agreement with the measured data.

3 Results and discussion

The discussion is divided into four Sections. First we will discuss the new temperature reconstruction in Sect. 3.1, followed by simple consideration of the $\delta^{15}\text{N}$ damping in the firn in Sect. 3.2. The used accumulation rate is reconsidered in Sect. 3.3 and finally we discuss the $\delta^{18}\text{O}_{\text{ice}}$ -temperature-relationship in Sects. 3.3.1 and 3.3.2.

3.1 Temperature

The reconstructed NGRIP temperature evolution from 10 kyr to 120 kyr b2k, together with the used $\delta^{18}\text{O}_{\text{ice}}$ data and the measured and modelled $\delta^{15}\text{N}$ data, is shown in Fig. 2. The 2 sigma uncertainty linked to a temperature increase at the onset of a DO event is $\pm 3^\circ\text{C}$ (Huber et al., 2006b). The temperature evolution for the transition Younger Dryas-Holocene (DO 0) to DO 8 is presented here the first time whereas the temperature evolution for DO 9 to DO 25 is a reanalysis of existing data. Caution should be taken in the interpretation in the two temperature bumps occurring at around 80 kyr and 100 kyr, where the shape of the temperature curve differs noticeably from the one of the $\delta^{18}\text{O}_{\text{ice}}$ signal (see Sect. 3.3).

To define the temperature amplitude of a DO event we had to specify the onset and end of the event. The criterion to define the onset of a DO event corresponds to the difference quotient exceeding $0.25^\circ\text{C}/50\text{ yr}$ ($0.05^\circ\text{C decade}^{-1}$), which is equivalent to about one-tenth of the increase rates for DO 9 to 17 found by Huber et al. (2006b). The end of the event was determined likewise, i.e. when the temperature increase rate became smaller than $0.05^\circ\text{C decade}^{-1}$. The 50 yr time interval was chosen because it

NGRIP temperature reconstruction from 10 to 120 kyr b2k

P. Kindler et al.

Title Page

Abstract

Introduction

Conclusions

References

Tables

Figures



Back

Close

Full Screen / Esc

Printer-friendly Version

Interactive Discussion



is long enough to overcome small-scale temperature variations. When one would use a longer time interval of 100 yr or longer, the durations of the temperature increases tend to be prolonged in an unrealistic way and the corresponding temperature amplitudes are in general slightly reduced.

5 With this method, we could well identify the start and end point of a DO event in general. For the determination of the temperature amplitude at DO events, which feature a two-step temperature increase, we had to apply the above mentioned criterion slightly differently. Examples for such DO events are DO 2, 7 (Fig. 2c), 11 and 18. The duration of the small drop in temperature generally lasts for less than 100 yr and the amplitudes of less than 1 °C are quite small. As both sections of such a split temperature increase exhibit about the same temperature increase rate they were treated as one increase, which means that the criterion of the 0.05 °C per decade was not applied during these small temperature reversals in between. Also DO 9 features basically a stop (Fig. 2d). As the temperature plateau in this reconstruction is of longer duration (about 300 yr) than the following temperature increase (140 yr), the temperature plateau was not taken into account in our evaluation which leads to a $\Delta t = 140$ yr and $\Delta T = 6.5$ °C. This is lower in amplitude than the findings from Huber et al. (2006b) that would be better in line when one includes the plateau resulting in $\Delta t = 564$ yr and $\Delta T = 8$ °C. DO 5 may (Fig. 2b) also be considered to have a small temperature reversal at the beginning when one includes the 2 °C temperature drop just before the onset of the DO event, resulting in $\Delta t = 473$ yr and $\Delta T = 14.5$ °C for DO 5. But when one looks closer to the onset of the DO event, the temperature reversal appears more to be some sort of plateau with a length of nearly 200 yr and the following temperature increase starts more gradual which is not the case in the temperature reversals of DO events mentioned above. So we exclude the small temperature drop before DO 5 from our temperature increase calculations.

20 Another type of temperature increase can be observed on DO 8, 12, 22 and maybe 17 where a slight long-term warming occurs before the start of the rapid temperature increase. They are roughly 3.5 °C in 950 yr (DO 8), 3 °C in 1300 yr (DO 12), 1 °C in

NGRIP temperature reconstruction from 10 to 120 kyr b2k

P. Kindler et al.

[Title Page](#)[Abstract](#)[Introduction](#)[Conclusions](#)[References](#)[Tables](#)[Figures](#)[Back](#)[Close](#)[Full Screen / Esc](#)[Printer-friendly Version](#)[Interactive Discussion](#)

NGRIP temperature reconstruction from 10 to 120 kyr b2k

P. Kindler et al.

[Title Page](#)[Abstract](#)[Introduction](#)[Conclusions](#)[References](#)[Tables](#)[Figures](#)[Back](#)[Close](#)[Full Screen / Esc](#)[Printer-friendly Version](#)[Interactive Discussion](#)

3500 yr (DO 17) and 2°C in 2800 yr (DO 22). The long term warming before DO 8 is comparable to the findings of Huber et al. (2006b) whereas they find a more pronounced long term warming of about 3 to 4°C for DO 17. It is interesting to note that before each of the DO events in marine isotope stage (MIS) 3 which exhibit first a long-term warming a Heinrich event took place (H4, H5 and H6). This feature is shown in Fig. 2 by the stadials marked with an orange background. Note that the colouring does not indicate the H events itself but the stadial where the event took place. The yellow shaded stadials, situated around the last glacial maximum, experience H events but do not manifest a long term warming before a DO event. The long term warming during H stadial 4 (before DO event 8) could be related to the findings of Jonkers et al. (2010), who investigated northern North Atlantic (near) sea surface temperatures based on marine sediment cores during MIS 3. They observe a slight sea surface temperature increase during peak-ice rafting at H event 4 and probably also H event 5 and suggest that warm water from a subsurface heat reservoir reached episodically the surface during the warmer period of the year. The feature of a Greenland long term warming during H stadial 4 could be of larger spatial extent as also Guillevic et al. (2013) found a slight long term warming during H stadial 4 at the NEEM site. Despite the fact that H events feature climatic changes in Europe (Genty et al., 2010; Sánchez Goñi et al., 2000), no particularly cold temperatures can be observed in our NGRIP temperature reconstruction during these stadial periods.

A linear relationship is observed between the length of the Greenland stadial and the temperature increase amplitude of the following AIM in Antarctica (EPICA community members, 2006; Capron et al., 2010a; Vallelonga et al., 2012). However, we do not observe a correlation between NGRIP temperature amplitudes and the duration of the preceding Greenland stadial (as defined by Capron et al., 2010a), or with the Antarctic EDML temperature rise (Stenni et al., 2010; EPICA community members, 2006). This finding of the inexistent correlation remains valid when using the preceding Greenland stadial and interstadial duration (instead of the stadial duration only). This behaviour suggests that the Greenland DO temperature amplitudes do not (only) depend on the

seesaw mechanism (Stocker and Johnsen, 2003) but are (also) governed by local effects. Sea ice cover in the Arctic retreating during the DO warming may be a good candidate, as suggested by Gildor and Tziperman (2003) and Li et al. (2010).

Generally, the DO events feature temperature amplitudes between 9 and 13°C which are independent of the background of the climate state (different MIS). The smallest temperature amplitude of 5°C is obtained for DO 25. This is 2 degrees more than the result from Capron et al. (2012) but within their uncertainty of $\pm 2.5^\circ\text{C}$. On the other hand the largest amplitude of our temperature reconstruction is DO 11 with 16.5°C, where Huber et al. (2006b) found a slightly smaller rise of 15°C but still within the given uncertainty. Capron et al. (2010a) mentioned abrupt cooling events within DO event 24, these variations, according to our finding, can exceed 10°C in about 150 yr.

Deviations of our temperature reconstruction compared to other studies using the $\delta^{15}\text{N}$ method can be explained by the application of different models (e.g. Goujon model, Goujon et al., 2003) and their adjustment to the measured data or by using a different approach, e.g. the combined use of $\delta^{15}\text{N}$ and $\delta^{40}\text{Ar}$ (Severinghaus et al., 1998; Landais et al., 2004b; Kobashi et al., 2011).

3.2 Damping of the $\delta^{15}\text{N}$ signal in the firn

Thomas et al. (2009) and Steffensen et al. (2008) investigated some transitions from stadials to interstadials on NGRIP ice using high resolution data (0.2 to 5 cm, corresponding to 3 yr or less) and found that some of these shifts can occur within a very short time period. The warming seen in the $\delta^{18}\text{O}_{\text{ice}}$ signal at DO 1 occurred within 3 yr (Steffensen et al., 2008) and the transition into the interstadial at DO 8 within 21 yr (Thomas et al., 2009). However, such rapid temperature increases cannot be seen in our temperature reconstruction. This may have two reasons: (i) as it is explained above, the $\delta^{18}\text{O}_{\text{ice}}$ data, which is used in the model input for a first temperature estimate, has a bag-resolution of 55 cm (corresponding to 10 to 100 yr) and is splined with a COP of 200 yr in order to reduce the signal variability in the firn densification and heat diffusion model to a level, which is in agreement with the measured $\delta^{15}\text{N}$ profile.

NGRIP temperature reconstruction from 10 to 120 kyr b2k

P. Kindler et al.

Title Page

Abstract

Introduction

Conclusions

References

Tables

Figures



Back

Close

Full Screen / Esc

Printer-friendly Version

Interactive Discussion



NGRIP temperature reconstruction from 10 to 120 kyr b2k

P. Kindler et al.

[Title Page](#)[Abstract](#)[Introduction](#)[Conclusions](#)[References](#)[Tables](#)[Figures](#)[Back](#)[Close](#)[Full Screen / Esc](#)[Printer-friendly Version](#)[Interactive Discussion](#)

to depths where the bubbles are enclosed altering the snow structure and therefore also the age distribution (Fig. 3b). Nevertheless, we accept this incompleteness in our simple calculation because at the time of the occurrence of the signal peak the temperature at the LID has only moderately changed. To allow for a small temperature rise at the LID we use in our calculations an age distribution corresponding to -45°C , slightly higher than the original temperature of -46°C . With these assumptions we find that for the considered scenario ($+10^{\circ}\text{C}$ in 20 yr) the signal amplitude is damped by roughly 30 % due to the gradual bubble enclosure process compared to the signal after the diffusion into the firn.

To compare the results of our simplified model calculations, we added measured $\delta^{15}\text{N}$ values of DO 8 both from NGRIP (green diamonds) and NEEM (violet diamonds), where a temperature increase of $8.8 \pm 1.2^{\circ}\text{C}$ has been found (Guillevic et al., 2013). Note that the y-axes of the NGRIP and NEEM $\delta^{15}\text{N}$ data have the same scale width compared to the y-axes of the modelled data but are shifted vertically in order to compare the shape of the signal evolution with the model simulations. The reason for the vertical offset of the data can be found in the gravitational part of the $\delta^{15}\text{N}$, which is a characteristic of the individual firn depth of the site. To get an estimate of the sensitivity of the damping we added the light blue solid lines which represent the signal after the gradual bubble enclosure of a $+7$ and $+13^{\circ}\text{C}$ temperature rise, respectively, according to our uncertainty of $\pm 3^{\circ}\text{C}$ of the temperature increase reconstruction.

As the measured data agree well with the shape of the solid lines, our simplified calculations indeed suggest a significant damping of the signal amplitude of roughly -30% due to the gradual bubble enclosure in the considered case. We refrain from calculating the damping of longer temperature increases because of the added uncertainty due to the more increased temperature at the LID which complicates the estimation of an appropriate age distribution. In general, it can be said that the damping decreases with increasing length of a temperature rise as well as with a smaller temperature amplitude and vice versa.

NGRIP temperature reconstruction from 10 to 120 kyr b2k

P. Kindler et al.

[Title Page](#)[Abstract](#)[Introduction](#)[Conclusions](#)[References](#)[Tables](#)[Figures](#)[⏪](#)[⏩](#)[◀](#)[▶](#)[Back](#)[Close](#)[Full Screen / Esc](#)[Printer-friendly Version](#)[Interactive Discussion](#)

Also shown in Fig. 3a is the grey line which represents the $\delta^{15}\text{N}$ signal as calculated by the Schwander model when the input data of the $+10^\circ\text{C}$ temperature increase is splined by 200 yr. One can see that the effect of this initial smoothing of the input data (possibility (i) mentioned above), which was introduced to reduce the variability in the model output, is of similar magnitude as the effect arising from the signal damping in the firn (possibility (ii)). Therefore we are confident that our reconstruction of the temperature amplitudes is still valid within the given uncertainty. This should also apply for other studies (Capron et al., 2010a; Guillevic et al., 2013; Huber et al., 2006b; Landais et al., 2005) where $\delta^{18}\text{O}_{\text{ice}}$ data smoothed up to 70 yr was used to estimate the corresponding site temperature.

For future work it is advisable to investigate the $\delta^{15}\text{N}$ damping in the firn in more detail with transient models and a highly resolved measurement of an exemplary DO event (e.g. DO 1, 5, 8 or 19). Additionally, it would make sense to implement a gradual bubble enclosure process in firn densification and heat diffusion models which are currently used to reconstruct the temperature evolution of a specific site. Also the calculations for $\delta^{15}\text{N}_{\text{therm}}$ should be further refined in these models since the temperature gradient, which is important for the determination of the $\delta^{15}\text{N}_{\text{therm}}$, currently depends only on two temperature points (top and bottom) and not on the actual temperature gradient itself. By this, the model may overestimate the $\delta^{15}\text{N}_{\text{therm}}$ at the beginning of a temperature increase.

3.3 Accumulation rate

As mentioned in Sect. 2.2 and illustrated in Fig. 4, we had to significantly reduce the accumulation rate in some parts to adjust the modelled $\delta^{15}\text{N}$ as well as Δdepth and Δage to match the measured ones. From 12 to 64 kyr the accumulation was lowered by 20 to 30 % with a mean value of 24 %, from 64 to 92 kyr by 0 to 10 % with a mean value of 5 % and from 92 to 123 kyr by 0 to 20 % with a mean value of 15 %. During some few short periods the accumulation rate was even reduced by 35 to 40 %.

NGRIP temperature reconstruction from 10 to 120 kyr b2k

P. Kindler et al.

Title Page

Abstract

Introduction

Conclusions

References

Tables

Figures

⏪

⏩

◀

▶

Back

Close

Full Screen / Esc

Printer-friendly Version

Interactive Discussion



A comparison of our temperature reconstruction with reduced accumulation to a scenario with unchanged accumulation is shown in Fig. 4. The red lines show the used reduced accumulation rate and the corresponding modelled Δ_{age} and Δ_{depth} values whereas the blue lines are obtained with an unchanged accumulation rate as described above in the Sect. 2.2 but without a final manual adjustment which would lead only to minor changes regarding Δ_{age} and Δ_{depth} values. One can clearly see that in the period from 10 to 60 kyr the 100%-accumulation-scenario underestimates the Δ_{age} by 50 to 500 yr and the Δ_{depth} up to 8 m. Most significant deviations occur during the last glacial maximum. Not shown is the modelled $\delta^{15}\text{N}$ data for the 100% accumulation rate-scenario, for which a substantial disagreement in the timing between measured and modelled data occurs in this corresponding period (modelled $\delta^{15}\text{N}$ values are shifted to younger ages). According to our data adjustment, the accumulation reduction seems to be smaller in the older half of the record, nevertheless also here our model suggests in some periods (around 69, 83, 96 and 119 kyr, marked with grey bars in Fig. 4) a major reduction of 30 to 40 %.

A general test concerning accumulation rates and corresponding LID (which influence the Δ_{age} and Δ_{depth}) can be performed with the Schwander model (Schwander et al., 1997). With the present-day NGRIP accumulation rate of 0.19 m i.e. yr⁻¹ and a mean temperature of -31.5 °C (NGRIP members, 2004), the Schwander model (Schwander et al., 1997) calculates a LID of 66.8 m, which is in excellent agreement to measurements of 66 to 68 m (Huber et al., 2006a). Consequently, in absence of any warming event, the model is also able to calculate the $\delta^{15}\text{N}_{\text{grav}}$. According to Figs. 2 and 4, the coldest temperatures of the reconstruction are around -55 °C and the lowest accumulation rates are in the order of 4 cm i.e. yr⁻¹. These are about the same values for Dome C present-day conditions: accumulation 2.7 cm i.e. yr⁻¹ and a temperature of -54.5 °C (Landais et al., 2006). So we can consider the Dome C characteristics as a test for the Schwander model for NGRIP lower boundary stadial conditions. When one runs the Schwander model with Dome C present-day conditions it is able to reproduce the LID (94.6 m) and the $\delta^{15}\text{N}_{\text{grav}}$ (0.51 ‰) well compared to observations of

LID = 98 m and $\delta^{15}\text{N}_{\text{grav}} = 0.52 \text{ ‰}$ (Landais et al., 2006). Therefore we are confident that the Schwander model is capable of modelling NGRIP glacial climatic conditions and we suggest that the Dansgaard–Johnsen ice flow model (Dansgaard and Johnsen, 1969; NGRIP members, 2004) which was used to establish the NGRIP accumulation rate probably provides generally too high glacial accumulation rates, especially during the coldest periods.

The fact that one has to reduce the NGRIP accumulation rate in some parts is not new. To reconstruct the temperature evolution from DO 9 to 17 (38 kyr to 64 kyr) Huber et al. (2006b) reduced the accumulation rate from the ss09sea06bm time scale constantly by 20 %. When one averages our time dependent reduced accumulation rate over the same period we get a similar value of 21.5 %. To test the validity of their model, Huber et al. (2006b) also modelled $\delta^{15}\text{N}$ values of DO 18 to 20 (64 kyr to 79 kyr) measured by Landais et al. (2004a) and found that in this period one can use mostly the unchanged accumulation rate, which is also in line with our findings. Also Guillevic et al. (2013) who reconstructed the NGRIP temperature on DO 8, 9 and 10 (36.5 to 43 kyr on the GICC05 time scale), using the same $\delta^{15}\text{N}$ data but the Goujon firnification model (Goujon et al., 2003), had to reduce the accumulation rate by 26 % in this section. Again, when averaged we find for the same period a similar accumulation reduction of 28 %. Interestingly, Landais et al. (2004a, 2005) and Capron et al. (2010a, 2012) worked with the original accumulation rate to reconstruct the temperature evolution over DO 18 to 25. These findings are mostly confirmed by our work where we use accumulation rates of approximately 100 % around the DO events mentioned above. An exception is DO 24 for which we had to lower the accumulation rate by around 20 %.

Back to 64 kyr, the ss09sea06bm time scale has been validated by the GICC05 annual layer counting time scale (Svensson et al., 2008), so in that time period the accumulation reduction cannot be due to inaccuracy in the time scale, but may likely be due to a too simplistic Dansgaard–Johnsen ice flow model (Guillevic et al., 2013). Our findings point in the same direction.

NGRIP temperature reconstruction from 10 to 120 kyr b2k

P. Kindler et al.

[Title Page](#)[Abstract](#)[Introduction](#)[Conclusions](#)[References](#)[Tables](#)[Figures](#)[⏪](#)[⏩](#)[◀](#)[▶](#)[Back](#)[Close](#)[Full Screen / Esc](#)[Printer-friendly Version](#)[Interactive Discussion](#)

NGRIP temperature reconstruction from 10 to 120 kyr b2k

P. Kindler et al.

[Title Page](#)[Abstract](#)[Introduction](#)[Conclusions](#)[References](#)[Tables](#)[Figures](#)[Back](#)[Close](#)[Full Screen / Esc](#)[Printer-friendly Version](#)[Interactive Discussion](#)

As mentioned above, we had to significantly reduce the accumulation rate in the older half of the record during some periods (grey bars in Fig. 4). The decreased accumulation rate leads to an increase in the modelled Δage , Δdepth (and temperature) in the corresponding periods (Figs. 4 and 5). Unfortunately, common $\delta^{15}\text{N}$ and $\delta^{18}\text{O}_{\text{ice}}$ signals are missing. Therefore we are not able to check our modelled Δage , Δdepth with measured data in these intervals. However, an indirect proxy for low accumulation rates is the dust content in the ice which shows in general elevated values during colder periods (Ruth et al., 2003) which are associated with low accumulation rates. Two of the four questionable low accumulation periods (83 and 96 kyr) mentioned above can be checked by dust data and are shown in Fig. 5 with grey bars on a depth scale. As in Fig. 4 the blue line represents the unchanged accumulation and the red line the used reduced accumulation rate, respectively. The dust content is shown in black on a logarithmic scale and the modelled Δage in orange, green dots represent Δage measurements. Highlighted with light blue one can see periods where low temperature and low accumulation rates are accompanied with clearly elevated dust contents. However, this is not the case in the grey shaded periods although our modelled accumulation rates are as low as or lower than those of the stadial between DO 21 and 22 (shown by dashed line). A potential explanation for our accumulation reduction could be an overestimation of the time duration of these periods by the ss09sea06bm timescale. One can see in Veres et al. (2012) that the duration of the long DO 23, where we found the most significant accumulation reduction, is about 1700 yr shorter on the new AICC 2012 time scale compared to the used ss09sea06bm time scale, probably because of a poorly determined thinning function near the bedrock (Veres et al., 2012). So, due to the fact that we were unable to confirm these four periods of low accumulation by the help of Δage and/or dust, caution should be taken by interpreting our accumulation rate (and temperature reconstruction) during these four time intervals.

NGRIP temperature reconstruction from 10 to 120 kyr b2k

P. Kindler et al.

[Title Page](#)[Abstract](#)[Introduction](#)[Conclusions](#)[References](#)[Tables](#)[Figures](#)[⏪](#)[⏩](#)[◀](#)[▶](#)[Back](#)[Close](#)[Full Screen / Esc](#)[Printer-friendly Version](#)[Interactive Discussion](#)

et al., 2005). This effect is incorporated in the top graph of Fig. 6, where the $\delta^{18}\text{O}_{\text{icecorr}}$ -temperature relationship data for the whole last glacial (15 to 119 kyr) is shown. The grey line indicates the modern Greenland spatial dependency of $\alpha = 0.80\text{‰}\cdot\text{C}^{-1}$ between $\delta^{18}\text{O}_{\text{ice}}$ and temperature (Sjolte et al., 2011), the black line shows the glacial $\delta^{18}\text{O}_{\text{icecorr}}$ -temperature relationship calculated by the geometric mean regression method. The green and the red diamond represent glacial and modern mean values, respectively. As described in Huber et al. (2006b) and as we suggest it is the case in an interstadial, a precipitation source temperature cooling would shift the grey line to the left (dashed grey line), which means that less depleted precipitation is expected. This can be understood by the help of a simple Rayleigh model: as the source temperature gets colder when its location shifts towards north, the temperature gradient (and also the precipitation transportation distance) between source and site is smaller and therefore the isotopic composition is less depleted. The source temperature cooling during interstadials is likely to be caused by the sea ice retreating around Greenland which allows high latitude water to evaporate and to serve as a Greenland precipitation source (Masson-Delmotte et al., 2005). This shift to higher expected $\delta^{18}\text{O}_{\text{ice}}$ values during the interstadial is indicated in Fig. 6 by the blue line. Compared to Huber et al. (2006b), we suggest a slightly different behaviour of the isotopic precipitation during stadial conditions. As the sea ice extent is enlarged during stadial conditions (Broecker, 2000), the precipitation source location for Greenland precipitation is pushed southwards to warmer ocean conditions which can be traced in the d-excess (Masson-Delmotte et al., 2005). In addition to the lower stadial $\delta^{18}\text{O}_{\text{ice}}$ values the expected isotopy should be further depleted because of the increased temperature gradient between precipitation source and the NGRIP site (Rayleigh), this suggested behaviour is shown in Fig. 6 by the red line. From that point of view, the discrepancy between observed and expected $\delta^{18}\text{O}_{\text{ice}}$ values is even enlarged. We therefore propose that the seasonality effect during stadials which is used to explain the mismatch between measured data and expected isotopic values is even more pronounced than previously thought.

3.3.2 Orbital control of the $\delta^{18}\text{O}_{\text{ice}}$ -temperature-sensitivity

Here we investigate the $\delta^{18}\text{O}_{\text{ice}}$ -temperature relationship at orbital time scales. For this, we calculated α ($\delta^{18}\text{O}_{\text{icecorr}}$ -temperature-relationship) on a 10 kyr time window, every 2 kyr (Fig. 7a), together with the corresponding correlation coefficient (R^2). Blue dots correspond to time windows with a robust correlation ($R^2 > 0.70$) and black dots to time windows with a weaker correlation ($0.47 < R^2 < 0.70$), occurring generally in time periods with rare and small abrupt climatic changes. The calculated α variations closely follow obliquity (Fig. 7a, green line, Berger and Loutre, 1991); α minima (around 0.3) correspond to obliquity maxima while alpha values reach up to 0.7 during obliquity minima. When looking at single DO events (1 kyr time window ending at the DO peak, small grey diamonds in Fig. 7a), the variations are more scattered and the α -obliquity relationship is almost impossible to detect.

Vimeux et al. (1999) for Antarctica and Masson-Delmotte et al. (2005) for Greenland evidenced the imprint of obliquity in the source-site temperature gradient as visible in the d-excess records of polar ice cores. Indeed, a low obliquity implies an increase of the source temperature and a cooling of the northern latitudes. The NGRIP $\delta^{18}\text{O}_{\text{ice}}$ record and our reconstructed temperature profile (10 kyr spline, Fig. 7a, red line) clearly show minima in phase with obliquity minima. Cold Greenland temperature during obliquity minima is most probably further reduced by positive feedbacks such as extending sea ice and albedo effects resulting in a further increase of the source-site temperature gradient.

The anticorrelation between α and obliquity that we observe cannot be explained by considering only the seasonality of the precipitation as in Masson-Delmotte et al. (2005) or Landais et al. (2004a). Indeed, in these studies, it is assumed that larger ice sheet (favoured by smaller obliquity) will strongly reduce the arrival of precipitation in winter and hence increase the seasonality effect, thus decreasing α . We observe the opposite: α is increasing with decreasing obliquity (Fig. 7a).

NGRIP temperature reconstruction from 10 to 120 kyr b2k

P. Kindler et al.

[Title Page](#)[Abstract](#)[Introduction](#)[Conclusions](#)[References](#)[Tables](#)[Figures](#)[Back](#)[Close](#)[Full Screen / Esc](#)[Printer-friendly Version](#)[Interactive Discussion](#)

We suggest that the observed α -obliquity-relationship can be explained by a schematic Rayleigh distillation model (Fig. 7b), where the $\delta^{18}\text{O}$ of precipitation is mainly explained by the source-site temperature gradient. In the case of an obliquity decrease, we move on the Rayleigh precipitation curve from the right black dot to the left one, which exhibits a steeper gradient (Fig. 7b, blue line). This steeper gradient would produce an enhanced isotopic effect for the same temperature variation in Greenland, increasing α , which would be in agreement with our observations.

Interestingly, the amplitude of α variations and the northern hemispheric ice sheets volume (Fig. 7a, black line, Bintanja et al., 2005) exhibit a concomitant increase from the Eemian to the Last Glacial Maximum. Note that the time uncertainty related to ice sheet size data is 4 kyr (Lisiecki and Raymo, 2005). We therefore suggest that during obliquity minima, α maxima are modulated by ice sheet size.

Moreover, while obliquity (and therefore also temperature) and α appear to be in phase at the beginning of the glacial period (110 kyr), one can observe an increasing lag of the α variations behind obliquity during the course of the glacial period ending in a lag of roughly 10 kyr at 30 kyr. Note that calculating α with different time windows (from 5 to 10 kyr) only slightly changes the position of the α peak at 20 kyr (± 0.9 kyr). Using $\delta^{18}\text{O}$ benthic data, Bintanja et al. (2005) and Waelbroeck et al. (2002) reconstructed the maximum ice sheet volume (or minimum sea-level) to be at around 20 kyr, where the dating uncertainty is ± 0.5 to 0.8 kyr (Waelbroeck et al., 2002). Taking into account the scatter in the different $\delta^{18}\text{O}$ benthic records, a maximum uncertainty of ± 4 kyr seems reasonable. The $\delta^{18}\text{O}$ benthic lag compared to obliquity is still bigger than this uncertainty. Since the time lag of α and ice sheet volume appear to be similar within dating uncertainty, this first continuous record of α over a complete glacial-interglacial cycle confirms that Northern Hemisphere ice sheet volume influences the hydrological cycle and therefore the $\delta^{18}\text{O}$ of precipitation. Werner et al. (2001) and Bromwich et al. (2004) suggested that the Laurentide ice sheet modified the air mass trajectories, possibly influencing Greenland by very depleted precipitation coming from Pacific sources. Again considering a simple Rayleigh model, these precipitations would (i) lower the

model partly overestimates the NGRIP accumulation rate (Dansgaard and Johnsen, 1969; NGRIP members, 2004).

When comparing the $\delta^{18}\text{O}_{\text{icecorr}}$ data with the corresponding temperatures during the last glacial and taking into account a warmer source temperature for the precipitation during stadials we propose that the seasonality effect of precipitation during stadials is even more pronounced than previously assumed. An anticorrelation between obliquity and a long term (10 kyr) α has been found. Qualitatively, this is supported by a simple Rayleigh distillation model. We suggest that the amplitudes of the α variations and their lag compared to obliquity are influenced by the northern hemispheric ice sheet volume. It would be interesting to use an isotopic model constrained by NGRIP isotopes and our reconstructed temperature to distinguish between the variations of α that can be explained by obliquity influencing the source-site temperature gradient (and thereby α), the ice-sheet volume effect and the variations that would remain unexplained (possibly influenced by seasonality of precipitations, storm trajectories and fluctuations of Arctic sea-ice extent).

Acknowledgements. We thank Peter Nyfeler and Hanspeter Moret for their helpful assistance during the measurements in the laboratory. This work is a contribution to the NGRIP ice core project, which is directed and organized by the Ice and Climate Research Group at the Niels Bohr Institute, University of Copenhagen. It is being supported by funding agencies in Denmark (SNF), Belgium (FNRS-CFB), France (IPEV, INSU/CNRS and ANR NEEM), Germany (AWI), Iceland (RannIs), Japan (MEXT), Sweden (SPRS), Switzerland (SNF) and the USA (NSF). This work was supported by the Swiss National Science Foundation contract No. 200020-135152.

NGRIP temperature reconstruction from 10 to 120 kyr b2k

P. Kindler et al.

Title Page

Abstract

Introduction

Conclusions

References

Tables

Figures



Back

Close

Full Screen / Esc

Printer-friendly Version

Interactive Discussion



References

- Alley, R., Anandakrishnan, S., and Jung, P.: Stochastic resonance in the North Atlantic, *Paleoceanography*, 16, 190–198, doi:10.1029/2000PA000518, 2001. 4102
- Andersen, K. K., Svensson, A., Johnsen, S. J., Rasmussen, S. O., Bigler, M., Röthlisberger, R., Ruth, U., Siggaard-Andersen, M.-L., Steffensen, J. P., Dahl-Jensen, D., Vinther, B. M., and Clausen, H. B.: The Greenland Ice Core Chronology 2005, 15–42 ka, Part 1: Constructing the time scale, *Quaternary Sci. Rev.*, 25, 3246–3257, doi:10.1016/j.quascirev.2006.08.002, 2006. 4107
- Berger, A. and Loutre, M.: Insolation Values for the Climate of the last 10 Million Years, *Quaternary Sci. Rev.*, 10, 297–317, doi:10.1016/0277-3791(91)90033-Q, 1991. 4121, 4143
- Bintanja, R., van de Wal, R., and Oerlemans, J.: Modelled atmospheric temperatures and global sea levels over the past million years, *Nature*, 437, 125–128, doi:10.1038/nature03975, 2005. 4119, 4122, 4143
- Blunier, T. and Brook, E.: Timing of millennial-scale climate change in Antarctica and Greenland during the last glacial period, *Science*, 291, 109–112, doi:10.1126/science.291.5501.109, 2001. 4103
- Bond, G., Broecker, W., Johnsen, S. J., MacManus, J., Laberrie, L., Jouzel, J., and Bonani, G.: Correlations between climate records from North Atlantic sediments and Greenland ice, *Nature*, 365, 143–147, doi:10.1038/365143a0, 1993. 4101, 4102
- Braun, H. and Kurths, J.: Were Dansgaard–Oeschger events forced by the sun?, *Eur. Phys. J.-Spec. Top.*, 191, 117–129, doi:10.1140/epjst/e2010-01345-5, 2010. 4102
- Braun, H., Christl, M., Rahmstorf, S., Ganopolski, A., Mangini, A., Kubatzki, C., Roth, K., and Kromer, B.: Possible solar origin of the 1,470-year glacial climate cycle demonstrated in a coupled model, *Nature*, 438, 208–211, doi:10.1038/nature04121, 2005. 4102
- Broecker, W.: Abrupt climate change: causal constraints provided by the paleoclimate record, *Earth-Sci. Rev.*, 51, 137–154, doi:10.1016/S0012-8252(00)00019-2, 2000. 4120
- Broecker, W., Peteet, D., and Rind, D.: Does the ocean-atmosphere system have more than one stable mode of operation?, *Nature*, 315, 21–26, doi:10.1038/315021a0, 1985. 4101
- Broecker, W. S., Bond, G., Klas, M., Bonani, G., and Wolfli, W.: A salt oscillator in the glacial Atlantic? 1. The concept, *Paleoceanography*, 5, 469–477, doi:10.1029/PA005i004p00469, 1990. 4101

NGRIP temperature reconstruction from 10 to 120 kyr b2k

P. Kindler et al.

Title Page

Abstract

Introduction

Conclusions

References

Tables

Figures



Back

Close

Full Screen / Esc

Printer-friendly Version

Interactive Discussion



NGRIP temperature reconstruction from 10 to 120 kyr b2k

P. Kindler et al.

Title Page

Abstract

Introduction

Conclusions

References

Tables

Figures



Back

Close

Full Screen / Esc

Printer-friendly Version

Interactive Discussion



- Bromwich, D., Toracinta, E., Wei, H., Oglesby, R., Fastook, J., and Hughes, T.: Polar MM5 simulations of the winter climate of the Laurentide Ice Sheet at the LGM, *J. Climate*, 17, 3415–3433, doi:10.1175/1520-0442(2004)017<3415:PMSOTW>2.0.CO;2, 2004. 4122
- Burns, S., Fleitmann, D., Matter, A., Kramers, J., and Al-Subbary, A.: Indian Ocean climate and an absolute chronology over Dansgaard/Oeschger events 9 to 13, *Science*, 301, 1365–1367, doi:10.1126/science.1086227, 2003. 4103
- Capron, E., Landais, A., Chappellaz, J., Schilt, A., Buiron, D., Dahl-Jensen, D., Johnsen, S. J., Jouzel, J., Lemieux-Dudon, B., Louergue, L., Leuenberger, M., Masson-Delmotte, V., Meyer, H., Oerter, H., and Stenni, B.: Millennial and sub-millennial scale climatic variations recorded in polar ice cores over the last glacial period, *Clim. Past*, 6, 345–365, doi:10.5194/cp-6-345-2010, 2010a. 4103, 4104, 4106, 4111, 4112, 4115, 4117, 4123, 4137
- Capron, E., Landais, A., Lemieux-Dudon, B., Schilt, A., Masson-Delmotte, V., Buiron, D., Chappellaz, J., Dahl-Jensen, D., Johnsen, S., Leuenberger, M., Louergue, L., and Oerter, H.: Synchronising EDML and NorthGRIP ice cores using $\delta^{18}\text{O}$ of atmospheric oxygen ($\delta^{18}\text{O}_{\text{atm}}$) and CH₄ measurements over MIS5 (80–123 kyr), *Quaternary Sci. Rev.*, 29, 222–234, doi:10.1016/j.quascirev.2009.07.014, 2010b. 4103, 4106, 4137
- Capron, E., Landais, A., Chappellaz, J., Buiron, D., Fischer, H., Johnsen, S. J., Jouzel, J., Leuenberger, M., Masson-Delmotte, V., and Stocker, T. F.: A global picture of the first abrupt climatic event occurring during the last glacial inception, *Geophys. Res. Lett.*, 39, L15703, doi:10.1029/2012GL052656, 2012. 4101, 4104, 4106, 4112, 4117, 4123, 4137
- Chiang, J. and Bitz, C.: Influence of high latitude ice cover on the marine Intertropical Convergence Zone, *Clim. Dynam.*, 25, 477–496, doi:10.1007/s00382-005-0040-5, 2005. 4103
- Craig, H., Horibe, Y., and Sowers, T.: Gravitational separation of gases and isotopes in polar ice caps, *Science*, 242, 1675–1678, doi:10.1126/science.242.4886.1675, 1988. 4105
- Dansgaard, W. and Johnsen, S. J.: A flow model and a time scale for the ice core from Camp Century, Greenland, *J. Glaciol.*, 8, 215–223, 1969. 4117, 4124
- Dansgaard, W., Clausen, H., Gundestrup, N., Hammer, C., Johnsen, S., Gristinsdottir, P., and Reeh, N.: A new Greenland deep ice core, *Science*, 218, 1273–1277, doi:10.1126/science.218.4579.1273, 1982. 4100
- Dansgaard, W., Johnsen, S., Clausen, H., Dahljensen, D., Gundestrup, N., Hammer, C., Hvidberg, C., Steffensen, J., Sveinbjornsdottir, A., Jouzel, J., and Bond, G.: Evidence for general instability of past climate from a 250-kyr ice-core record, *Nature*, 364, 218–220, doi:10.1038/364218a0, 1993. 4101

NGRIP temperature reconstruction from 10 to 120 kyr b2k

P. Kindler et al.

[Title Page](#)[Abstract](#)[Introduction](#)[Conclusions](#)[References](#)[Tables](#)[Figures](#)[Back](#)[Close](#)[Full Screen / Esc](#)[Printer-friendly Version](#)[Interactive Discussion](#)

- Deplazes, G., Lückge, A., Peterson, L. C., Timmermann, A., Hamann, Y., Hughen, K. A., Rühl, U., Laj, C., Cane, M. A., Sigman, D. M., and Haug, G. H.: Links between tropical rainfall and North Atlantic climate during the last glacial period, *Nat. Geosci.*, 6, 213–217, doi:10.1038/NGEO1712, 2013. 4101
- 5 Ditlevsen, P. D., Andersen, K. K., and Svensson, A.: The DO-climate events are probably noise induced: statistical investigation of the claimed 1470 years cycle, *Clim. Past*, 3, 129–134, doi:10.5194/cp-3-129-2007, 2007. 4102
- Elliot, M., Labeyrie, L., and Duplessy, J.: Changes in North Atlantic deep-water formation associated with the Dansgaard–Oeschger temperature oscillations (60–10 ka), *Quaternary Sci. Rev.*, 21, 1153–1165, doi:10.1016/S0277-3791(01)00137-8, 2002. 4102
- 10 EPICA community members: One-to-one coupling of glacial climate variability in Greenland and Antarctica, *Nature*, 444, 195–198, doi:10.1038/nature05301, 2006. 4103, 4111
- Fawcett, P. J., Agustdóttir, A. M., Alley, R. B., and Shuman, C. A.: The younger dryas termination and North Atlantic deep water formation: insights from climate model simulations and Greenland ice cores, *Paleoceanography*, 12, 23–38, doi:10.1029/96PA02711, 1997. 4119
- Fleitmann, D., Cheng, H., Badertscher, S., Edwards, R. L., Mudelsee, M., Goektuerk, O. M., Fankhauser, A., Pickering, R., Raible, C. C., Matter, A., Kramers, J., and Tuysuz, O.: Timing and climatic impact of Greenland interstadials recorded in stalagmites from northern Turkey, *Geophys. Res. Lett.*, 36, L19707, doi:10.1029/2009GL040050, 2009. 4101
- 20 Genty, D., Combourieu-Nebout, N., Peyron, O., Blamart, D., Wainer, K., Mansuri, F., Ghaleb, B., Isabello, L., Dormoy, I., von Grafenstein, U., Bonelli, S., Landais, A., and Brauer, A.: Isotopic characterization of rapid climatic events during OIS3 and OIS4 in Villars Cave stalagmites (SW-France) and correlation with Atlantic and Mediterranean pollen records, *Quaternary Sci. Rev.*, 29, 2799–2820, doi:10.1016/j.quascirev.2010.06.035, 2010. 4111
- 25 Gildor, H. and Tziperman, E.: Sea-ice switches and abrupt climate change, *Philos. T. Roy. Soc. A*, 361, 1935–1942, doi:10.1098/rsta.2003.1244, 2003. 4112, 4119
- Goujon, C., Barnola, J., and Ritz, C.: Modeling the densification of polar firn including heat diffusion: application to close-off characteristics and gas isotopic fractionation for Antarctica and Greenland sites, *J. Geophys. Res.*, 108, 4792, doi:10.1029/2002JD003319, 2003. 4112, 4113, 4117
- 30 Grachev, A. and Severinghaus, J.: A revised $+10 \pm 4^\circ\text{C}$ magnitude of the abrupt change in Greenland temperature at the Younger Dryas termination using published GISP2 gas

NGRIP temperature reconstruction from 10 to 120 kyr b2k

P. Kindler et al.

[Title Page](#)

[Abstract](#)

[Introduction](#)

[Conclusions](#)

[References](#)

[Tables](#)

[Figures](#)



[Back](#)

[Close](#)

[Full Screen / Esc](#)

[Printer-friendly Version](#)

[Interactive Discussion](#)



isotope data and air thermal diffusion constants, *Quaternary Sci. Rev.*, 24, 513–519, doi:10.1016/j.quascirev.2004.10.016, 2005. 4113

Guillevic, M., Bazin, L., Landais, A., Kindler, P., Orsi, A., Masson-Delmotte, V., Blunier, T., Buchardt, S. L., Capron, E., Leuenberger, M., Martinerie, P., Prié, F., and Vinther, B. M.: Spatial gradients of temperature, accumulation and $\delta^{18}\text{O}$ -ice in Greenland over a series of Dansgaard–Oeschger events, *Clim. Past*, 9, 1029–1051, doi:10.5194/cp-9-1029-2013, 2013. 4111, 4114, 4115, 4117, 4123, 4138

Heinrich, H.: Origin and consequences of cyclic ice rafting in the Northeast Atlantic Ocean during the past 130,000 years, *Quaternary Res.*, 29, 142–152, doi:10.1016/0033-5894(88)90057-9, 1988. 4102

Hemming, S.: Heinrich events: Massive late pleistocene detritus layers of the North Atlantic and their global climate imprint, *Rev. Geophys.*, 42, RG1005, doi:10.1029/2003RG000128, 2004. 4137

Huber, C. and Leuenberger, M.: Measurements of isotope and elemental ratios of air from polar ice with a new on-line extraction method, *Geochem. Geophys. Geosy.*, 5, Q10002, doi:10.1029/2004GC000766, 2004. 4106

Huber, C., Leuenberger, M., and Zumbrennen, O.: Continuous extraction of trapped air from bubble ice or water for on-line determination of isotope ratios, *Anal. Chem.*, 75, 2324–2332, doi:10.1021/ac0263972, 2003. 4106

Huber, C., Beyerle, U., Leuenberger, M., Schwander, J., Kipfer, R., Spahni, R., Severinghaus, J., and Weiler, K.: Evidence for molecular size dependent gas fractionation in firn air derived from noble gases, oxygen, and nitrogen measurements, *Earth Planet. Sc. Lett.*, 243, 61–73, doi:10.1016/j.epsl.2005.12.036, 2006a. 4116

Huber, C., Leuenberger, M., Spahni, R., Flückiger, J., Schwander, J., Stocker, T., Johnsen, S., Landais, A., and Jouzel, J.: Isotope calibrated Greenland temperature record over Marine Isotope Stage 3 and its relation to CH_4 , *Earth Planet. Sc. Lett.*, 243, 504–519, doi:10.1016/j.epsl.2006.01.002, 2006b. 4101, 4104, 4106, 4107, 4109, 4110, 4111, 4112, 4115, 4117, 4119, 4120, 4123, 4137

Johnsen, S., Dansgaard, W., Clausen, H., and Langway, C.: Oxygen isotope profiles through the Antarctic and Greenland ice sheets, *Nature*, 235, 429–434, 1972. 4100

Johnsen, S. J., Clausen, H. B., Dansgaard, W., Fuhrer, K., Gundestrup, N., Hammer, C. U., Iversen, P., Jouzel, J., Stauffer, B., and Steffensen, J. P.: Irregular glacial interstadials

recorded in a new Greenland ice core, *Nature*, 359, 311–313, doi:10.1038/359311a0, 1992. 4100

Johnsen, S. J., Dahl-Jensen, D., Gundestrup, N., Steffensen, J. P., Clausen, H. B., Miller, H., Masson-Delmotte, V., Sveinbjörnsdóttir, A., and White, J.: Oxygen isotope and palaeotemperature records from six Greenland ice-core stations: Camp Century, Dye-3, GRIP, GISP2, Renland and NorthGRIP, *J. Quaternary Sci.*, 16, 299–307, doi:10.1002/jqs.622, 2001. 4107

Jonkers, L., Moros, M., Prins, M. A., Dokken, T., Dahl, C. A., Dijkstra, N., Perner, K., and Brummer, G.-J. A.: A reconstruction of sea surface warming in the northern North Atlantic during MIS 3 ice-rafting events, *Quaternary Sci. Rev.*, 29, 1791–1800, doi:10.1016/j.quascirev.2010.03.014, 2010. 4111, 4137

Jouzel, J., Vimeux, F., Caillon, N., Delaygue, G., Hoffmann, G., Masson-Delmotte, V., and Parrenin, F.: Magnitude of isotope/temperature scaling for interpretation of central Antarctic ice cores, *J. Geophys. Res.-Atmos.*, 108, 4361, doi:10.1029/2002JD002677, 2003. 4119, 4142

Jouzel, J., Stievenard, N., Johnsen, S., Landais, A., Masson-Delmotte, V., Sveinbjörnsdóttir, A., Vimeux, F., von Grafenstein, U., and White, J.: The GRIP deuterium-excess record, *Quaternary Sci. Rev.*, 26, 1–17, doi:10.1016/j.quascirev.2006.07.015, 2007. 4119

Kanner, L. C., Burns, S. J., Cheng, H., and Edwards, R. L.: High-latitude forcing of the South American summer monsoon during the last glacial, *Science*, 335, 570–573, doi:10.1126/science.1213397, 2012. 4101, 4103

Kaspi, Y., Sayag, R., and Tziperman, E.: A “triple sea-ice state” mechanism for the abrupt warming and synchronous ice sheet collapses during Heinrich events, *Paleoceanography*, 19, PA3004, doi:10.1029/2004PA001009, 2004. 4119

Kobashi, T., Kawamura, K., Severinghaus, J. P., Barnola, J.-M., Nakaegawa, T., Vinther, B. M., Johnsen, S. J., and Box, J. E.: High variability of Greenland surface temperature over the past 4000 years estimated from trapped air in an ice core, *Geophys. Res. Lett.*, 38, L21501, doi:10.1029/2011GL049444, 2011. 4112

Krinner, G., Genthon, C., and Jouzel, J.: GCM analysis of local influences on ice core δ signals, *Geophys. Res. Lett.*, 24, 2825–2828, doi:10.1029/97GL52891, 1997. 4119

Landais, A., Caillon, N., Severinghaus, J., Jouzen, J., and Masson-Delmotte, V.: Analyses isotopiques à haute précision de l’air piégé dans les glaces polaires pour la quantification des variations rapides de température: méthode et limites, *Notes des Activités Instrumentales de l’IPSL*, nr. 39, 2003. 4106

CPD

9, 4099–4143, 2013

NGRIP temperature reconstruction from 10 to 120 kyr b2k

P. Kindler et al.

Title Page

Abstract

Introduction

Conclusions

References

Tables

Figures

◀

▶

◀

▶

Back

Close

Full Screen / Esc

Printer-friendly Version

Interactive Discussion



NGRIP temperature reconstruction from 10 to 120 kyr b2k

P. Kindler et al.

[Title Page](#)

[Abstract](#)

[Introduction](#)

[Conclusions](#)

[References](#)

[Tables](#)

[Figures](#)



[Back](#)

[Close](#)

[Full Screen / Esc](#)

[Printer-friendly Version](#)

[Interactive Discussion](#)

- Landais, A., Barnola, J., Masson-Delmotte, V., Jouzel, J., Chappellaz, J., Caillon, N., Huber, C., Leuenberger, M., and Johnsen, S.: A continuous record of temperature evolution over a sequence of Dansgaard–Oeschger events during Marine Isotopic Stage 4 (76 to 62 kyr BP), *Geophys. Res. Lett.*, 31, L22211, doi:10.1029/2004GL021193, 2004a. 4104, 4106, 4117, 4121, 4137
- Landais, A., Caillon, N., Goujon, C., Grachev, A., Barnola, J., Chappellaz, J., Jouzel, J., Masson-Delmotte, V., and Leuenberger, M.: Quantification of rapid temperature change during DO event 12 and phasing with methane inferred from air isotopic measurements, *Earth Planet. Sc. Lett.*, 225, 221–232, doi:10.1016/j.epsl.2004.06.009, 2004b. 4112
- Landais, A., Caillon, N., Severinghaus, J., Barnola, J., Goujon, C., Jouzel, J., and Masson-Delmotte, V.: Isotopic measurements of air trapped in ice to quantify temperature changes, *C. R. Geosci.*, 336, 963–970, doi:10.1016/j.crte.2004.03.013, 2004c. 4106
- Landais, A., Jouzel, J., Masson-Delmotte, V., and Caillon, N.: Large temperature variations over rapid climatic events in Greenland: a method based on air isotopic measurements, *C. R. Geosci.*, 337, 947–956, doi:10.1016/j.crte.2005.04.003, 2005. 4101, 4104, 4106, 4115, 4117, 4123, 4137
- Landais, A., Barnola, J., Kawamura, K., Caillon, N., Delmotte, M., Ommen, T. V., Dreyfus, G., Jouzel, J., Masson-Delmotte, V., Minster, B., Freitag, J., Leuenberger, M., Schwander, J., Huber, C., Etheridge, D., and Morgan, V.: Firn-air $\delta^{15}\text{N}$ in modern polar sites and glacial-interglacial ice: a model-data mismatch during glacial periods in Antarctica?, *Quaternary Sci. Rev.*, 25, 49–62, doi:10.1016/j.quascirev.2005.06.007, 2006. 4116, 4117
- Lang, C., Leuenberger, M., Schwander, J., and Johnsen, S.: 16°C rapid temperature variation in Central Greenland 70,000 years ago, *Science*, 286, 934–937, doi:10.1126/science.286.5441.934, 1999. 4101, 4104
- Leuenberger, M., Lang, C., and Schwander, J.: $\Delta^{15}\text{N}$ measurements as a calibration tool for the paleothermometer and gas-ice age differences: a case study for the 8200 BP event on GRIP ice, *J. Geophys. Res.-Atmos.*, 104, 22163–22170, doi:10.1029/1999JD900436, 1999. 4104, 4105
- Li, C., Battisti, D., Schrag, D., and Tziperman, E.: Abrupt climate shifts in Greenland due to displacements of the sea ice edge, *Geophys. Res. Lett.*, 32, L19702, doi:10.1029/2005GL023492, 2005. 4119

NGRIP temperature reconstruction from 10 to 120 kyr b2k

P. Kindler et al.

Title Page

Abstract

Introduction

Conclusions

References

Tables

Figures

◀

▶

◀

▶

Back

Close

Full Screen / Esc

Printer-friendly Version

Interactive Discussion

- Li, C., Battisti, D. S., and Bitz, C. M.: Can North Atlantic sea ice anomalies account for Dansgaard–Oeschger climate signals?, *J. Climate*, 23, 5457–5475, doi:10.1175/2010JCLI3409.1, 2010. 4102, 4112, 4119
- Lisiecki, L. and Raymo, M.: A Pliocene–Pleistocene stack of 57 globally distributed benthic $\delta^{18}\text{O}$ records, *Paleoceanography*, 20, PA1003, doi:10.1029/2004PA001071, 2005. 4119, 4122
- Masson-Delmotte, V., Jouzel, J., Landais, A., Stiévenard, M., Johnsen, S. J., White, J. W. C., Werner, M., Sveinbjörnsdóttir, A., and Fuhrer, K.: GRIP deuterium excess reveals rapid and orbital-scale changes in Greenland moisture origin, *Science*, 309, 118–121, doi:10.1126/science.1108575, 2005. 4119, 4120, 4121
- Mayewski, P., Meeker, L., Twickler, M., Whitlow, S., Yang, Q., Lyons, W., and Prentice, M.: Major features and forcing of high-latitude northern hemisphere atmospheric circulation using a 110,000-year-long glaciochemical series, *J. Geophys. Res.-Oceans*, 102, 26345–26366, doi:10.1029/96JC03365, 1997. 4101
- NGRIP members: High-resolution record of Northern Hemisphere climate extending into the last interglacial period, *Nature*, 431, 147–151, doi:10.1038/nature02805, 2004. 4101, 4104, 4107, 4116, 4117, 4124
- Paterson, W. S. B.: *The Physics of Glaciers*, Pergamon, Tarrytown, NY, 1994. 4105
- Petersen, S. V., Schrag, D. P., and Clark, P. U.: A new mechanism for Dansgaard–Oeschger cycles, *Paleoceanography*, doi:10.1029/2012PA002364, in press, 2013. 4102
- Rahmstorf, S.: Ocean circulation and climate during the past 120,000 years, *Nature*, 419, 207–214, doi:10.1038/nature01090, 2002. 4101
- Rasmussen, T. and Thomsen, E.: The role of the North Atlantic Drift in the millennial timescale glacial climate fluctuations, *Palaeogeogr. Palaeoclimatol.*, 210, 101–116, doi:10.1016/j.palaeo.2004.04.005, 2004. 4102
- Roche, D., Paillard, D., and Cortijo, E.: Constraints on the duration and freshwater release of Heinrich event 4 through isotope modelling, *Nature*, 432, 379–382, doi:10.1038/nature03059, 2004. 4137
- Ruth, U., Wagenbach, D., Steffensen, J., and Bigler, M.: Continuous record of microparticle concentration and size distribution in the central Greenland NGRIP ice core during the last glacial period, *J. Geophys. Res.-Atmos.*, 108, 4098, doi:10.1029/2002JD002376, 2003. 4101, 4118, 4140

NGRIP temperature reconstruction from 10 to 120 kyr b2k

P. Kindler et al.

Title Page

Abstract

Introduction

Conclusions

References

Tables

Figures



Back

Close

Full Screen / Esc

Printer-friendly Version

Interactive Discussion



Sánchez Goñi, M. F. and Harrison, S. P.: Millennial-scale climate variability and vegetation changes during the last glacial: concepts and terminology Introduction, *Quaternary Sci. Rev.*, 29, 2823–2827, doi:10.1016/j.quascirev.2009.11.014, 2010. 4137

Sánchez Goñi, M. F., Turon, J., Eynaud, F., and Gendreau, S.: European climatic response to millennial-scale changes in the atmosphere-ocean system during the last glacial period, *Quaternary Res.*, 54, 394–403, doi:10.1006/qres.2000.2176, 2000. 4111

Schilt, A., Baumgartner, M., Blunier, T., Schwander, J., Spahni, R., Fischer, H., and Stocker, T. F.: Glacial-interglacial and millennial-scale variations in the atmospheric nitrous oxide concentration during the last 800,000 years, *Quaternary Sci. Rev.*, 29, 182–192, doi:10.1016/j.quascirev.2009.03.011, 2010. 4101

Schwander, J.: The Transformation of snow to ice and the occlusion of gases, in: *The Environmental Record in Glaciers and Ice Sheets*, edited by: Oeschger, H. and Langway, C. C., Physical, Chemical, and Earth Sciences Research Reports, John Wiley, New York, 53–67, 1989. 4105

Schwander, J., Sowers, T., Barnola, J., Blunier, T., Fuchs, A., and Malaizé, B.: Age scale of the air in the summit ice: implication for glacial-interglacial temperature change, *J. Geophys. Res.-Atmos.*, 102, 19483–19493, doi:10.1029/97JD01309, 1997. 4104, 4107, 4113, 4116

Severinghaus, J., Sowers, T., Brook, E., Alley, R., and Bender, M.: Timing of abrupt climate change at the end of the younger dryas interval from thermally fractionated gases in polar ice, *Nature*, 391, 141–146, doi:10.1038/34346, 1998. 4101, 4104, 4105, 4112

Sjolte, J., Hoffmann, G., Johnsen, S. J., Vinther, B. M., Masson-Delmotte, V., and Sturm, C.: Modeling the water isotopes in Greenland precipitation 1959–2001 with the meso-scale model REMO-iso, *J. Geophys. Res.-Atmos.*, 116, D18105, doi:10.1029/2010JD015287, 2011. 4120, 4142

Spahni, R., Schwander, J., Flückiger, J., Stauffer, B., Chappellaz, J., and Raynaud, D.: The attenuation of fast atmospheric CH₄ variations recorded in polar ice cores, *Geophys. Res. Lett.*, 30, 1571, doi:10.1029/2003GL017093, 2003. 4113, 4138

Steffensen, J. P., Andersen, K. K., Bigler, M., Clausen, H. B., Dahl-Jensen, D., Fischer, H., Goto-Azuma, K., Hansson, M., Johnsen, S. J., Jouzel, J., Masson-Delmotte, V., Popp, T., Rasmussen, S. O., Röthlisberger, R., Ruth, U., Stauffer, B., Siggaard-Andersen, M.-L., Sveinbjörnsdóttir, A. E., Svensson, A., and White, J. W. C.: High-resolution Greenland ice core data show abrupt climate change happens in few years, *Science*, 321, 680–684, doi:10.1126/science.1157707, 2008. 4112

NGRIP temperature reconstruction from 10 to 120 kyr b2k

P. Kindler et al.

[Title Page](#)

[Abstract](#)

[Introduction](#)

[Conclusions](#)

[References](#)

[Tables](#)

[Figures](#)

[⏪](#)

[⏩](#)

[◀](#)

[▶](#)

[Back](#)

[Close](#)

[Full Screen / Esc](#)

[Printer-friendly Version](#)

[Interactive Discussion](#)

- Steig, E., Grootes, P., and Stuiver, M.: Seasonal precipitation timing and ice core records, *Science*, 266, 1885–1886, doi:10.1126/science.266.5192.1885, 1994. 4119
- Stenni, B., Masson-Delmotte, V., Selmo, E., Oerter, H., Meyer, H., Roethlisberger, R., Jouzel, J., Cattani, O., Falourd, S., Fischer, H., Hoffmann, G., Iacumin, P., Johnsen, S. J., Minster, B., and Udisti, R.: The deuterium excess records of EPICA Dome C and Dronning Maud Land ice cores (East Antarctica), *Quaternary Sci. Rev.*, 29, 146–159, doi:10.1016/j.quascirev.2009.10.009, 2010. 4103, 4111
- Stocker, T. and Johnsen, S.: A minimum thermodynamic model for the bipolar seesaw, *Paleoceanography*, 18, 1087, doi:10.1029/2003PA000920, 2003. 4103, 4112
- Svensson, A., Andersen, K. K., Bigler, M., Clausen, H. B., Dahl-Jensen, D., Davies, S. M., Johnsen, S. J., Muscheler, R., Parrenin, F., Rasmussen, S. O., Röthlisberger, R., Seierstad, I., Steffensen, J. P., and Vinther, B. M.: A 60 000 year Greenland stratigraphic ice core chronology, *Clim. Past*, 4, 47–57, doi:10.5194/cp-4-47-2008, 2008. 4117
- Thomas, E. R., Wolff, E. W., Mulvaney, R., Johnsen, S. J., Steffensen, J. P., and Arron-smith, C.: Anatomy of a Dansgaard–Oeschger warming transition: high-resolution analysis of the North Greenland Ice Core Project ice core, *J. Geophys. Res.-Atmos.*, 114, D08102, doi:10.1029/2008JD011215, 2009. 4112, 4113
- Vallelonga, P., Bertagna, G., Blunier, T., Kjær, H. A., Popp, T. J., Rasmussen, S. O., Steffensen, J. P., Stowasser, C., Svensson, A. S., Warming, E., Winstrup, M., Bigler, M., and Kipfstuhl, S.: Duration of Greenland Stadial 22 and ice-gas Δ age from counting of annual layers in Greenland NGRIP ice core, *Clim. Past*, 8, 1839–1847, doi:10.5194/cp-8-1839-2012, 2012. 4103, 4111
- Veres, D., Bazin, L., Landais, A., Toyé Mahamadou Kele, H., Lemieux-Dudon, B., Parrenin, F., Martinerie, P., Blayo, E., Blunier, T., Capron, E., Chappellaz, J., Rasmussen, S. O., Severi, M., Svensson, A., Vinther, B., and Wolff, E. W.: The Antarctic ice core chronology (AICC2012): an optimized multi-parameter and multi-site dating approach for the last 120 thousand years, *Clim. Past Discuss.*, 8, 6011–6049, doi:10.5194/cpd-8-6011-2012, 2012. 4118
- Vimeux, F., Masson, V., Jouzel, J., Stievenard, M., and Petit, J.: Glacial-interglacial changes in ocean surface conditions in the southern hemisphere, *Nature*, 398, 410–413, doi:10.1038/18860, 1999. 4121
- Waelbroeck, C., Labeyrie, L., Michel, E., Duplessy, J., McManus, J., Lambeck, K., Balbon, E., and Labracherie, M.: Sea-level and deep water temperature changes derived from ben-

thic foraminifera isotopic records, *Quaternary Sci. Rev.*, 21, 295–305, doi:10.1016/S0277-3791(01)00101-9, 2002. 4122

Wang, Y., Cheng, H., Edwards, R., An, Z., Wu, J., Shen, C., and Dorale, J.: A high-resolution absolute-dated Late Pleistocene monsoon record from Hulu Cave, China, *Science*, 294, 2345–2348, doi:10.1126/science.1064618, 2001. 4101, 4103

Werner, M., Heimann, M., and Hoffmann, G.: Isotopic composition and origin of polar precipitation in present and glacial climate simulations, *Tellus B*, 53, 53–71, doi:10.1034/j.1600-0889.2001.01154.x, 2001. 4122

Woillez, M.-N., Krinner, G., Kageyama, M., and Delaygue, G.: Impact of solar forcing on the surface mass balance of northern ice sheets for glacial conditions, *Earth Planet. Sc. Lett.*, 335, 18–24, doi:10.1016/j.epsl.2012.04.043, 2012. 4102

Wolff, E. W., Chappellaz, J., Blunier, T., Rasmussen, S. O., and Svensson, A.: Millennial-scale variability during the last glacial: the ice core record, *Quaternary Sci. Rev.*, 29, 2828–2838, doi:10.1016/j.quascirev.2009.10.013, 2010. 4103

CPD

9, 4099–4143, 2013

NGRIP temperature reconstruction from 10 to 120 kyr b2k

P. Kindler et al.

Title Page

Abstract

Introduction

Conclusions

References

Tables

Figures

⏪

⏩

◀

▶

Back

Close

Full Screen / Esc

Printer-friendly Version

Interactive Discussion



NGRIP temperature reconstruction from 10 to 120 kyr b2k

P. Kindler et al.

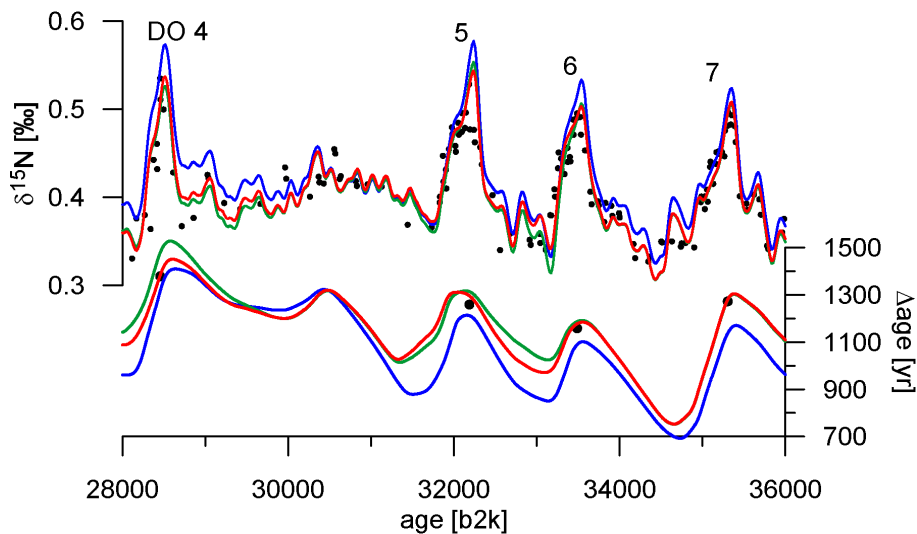
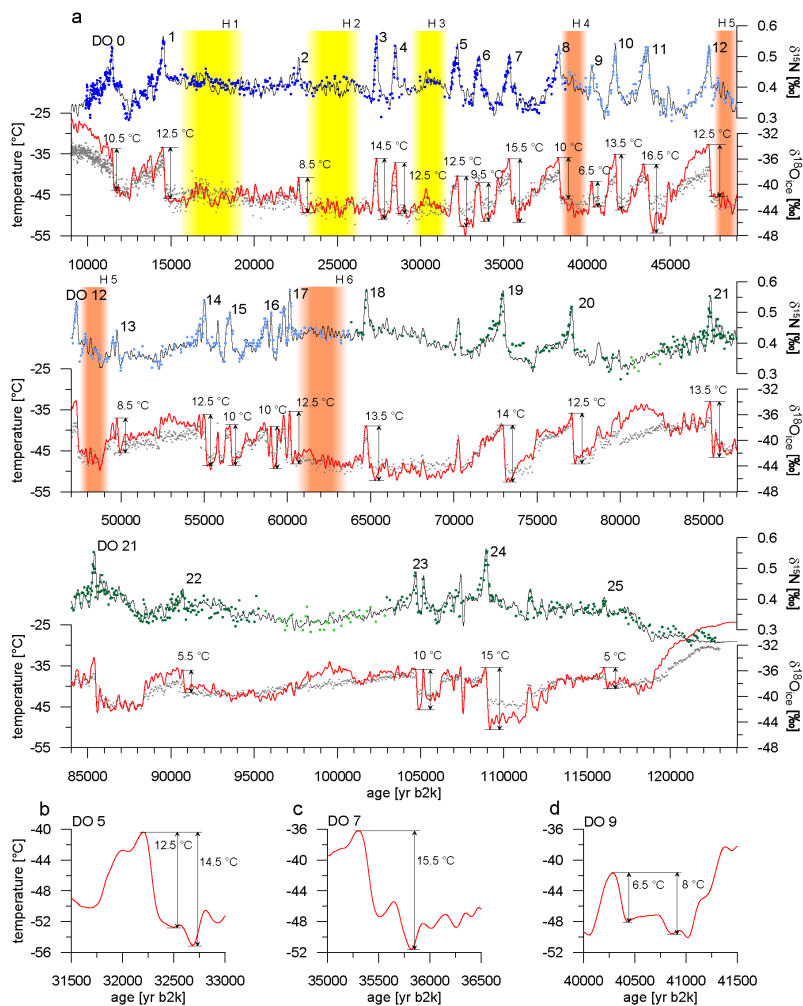


Fig. 1. The effects of the three steps of the temperature reconstruction on the modelled $\delta^{15}\text{N}$ and Δage are marked with three different colours on a gas age scale: step (i) (α adjustment) in blue, step (ii) (accumulation and temperature adjustment) in green and step (iii) (manual adjustment where needed) in red. Black dots are $\delta^{15}\text{N}$ and Δage measurements.

[Title Page](#)[Abstract](#)[Introduction](#)[Conclusions](#)[References](#)[Tables](#)[Figures](#)[Back](#)[Close](#)[Full Screen / Esc](#)[Printer-friendly Version](#)[Interactive Discussion](#)

NGRIP temperature reconstruction from 10 to 120 kyr b2k

P. Kindler et al.



Title Page

Abstract

Introduction

Conclusions

References

Tables

Figures



Back

Close

Full Screen / Esc

Printer-friendly Version

Interactive Discussion



Fig. 2. (a) NGRIP temperature reconstruction from 10 to 120 kyr b2k on the ss09sea06bm time scale. Red line: temperature reconstruction, grey points: $\delta^{18}\text{O}_{\text{ice}}$ (bag mean) on ice age scale, dark blue points: new $\delta^{15}\text{N}$ measurements, this study, light blue points: measurements from Huber et al. (2006b), dark green points: published $\delta^{15}\text{N}$ measurements from LSCE (Landais et al., 2004a, 2005; Capron et al., 2010b,a, 2012), light green points: unpublished $\delta^{15}\text{N}$ measurements from LSCE, black line: modelled $\delta^{15}\text{N}$, all $\delta^{15}\text{N}$ data are plotted on the gas age scale. Because there is no exact agreement in the literature about the timing and the duration of H events (Hemming, 2004; Sánchez Goñi and Harrison, 2010; Jonkers et al., 2010; Roche et al., 2004), we do not explicitly indicate the H events themselves but the stadials in which they took place by colouring the corresponding time period in yellow (no long term warming observed in the stadial with a H event) and orange (a long term warming is observed). **(b)–(d)** Focus on the temperature evolution of DO 5, 7 and 9.

NGRIP temperature reconstruction from 10 to 120 kyr b2k

P. Kindler et al.

[Title Page](#)[Abstract](#)[Introduction](#)[Conclusions](#)[References](#)[Tables](#)[Figures](#)[Back](#)[Close](#)[Full Screen / Esc](#)[Printer-friendly Version](#)[Interactive Discussion](#)

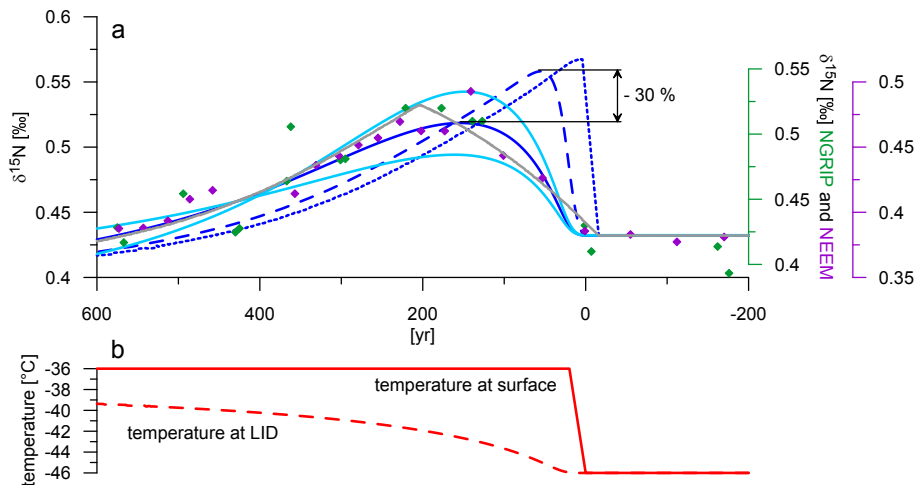


Fig. 3. Simplified model calculation for a possible $\delta^{15}\text{N}$ damping in the firn due to the gradual bubble enclosure for a rapid temperature increase within 20 yr. **(a)** The dark blue lines represent a scenario where a $+10^\circ\text{C}$ temperature increase (from -46 to -36°C) within 20 yr is assumed. The dotted line corresponds to the $\delta^{15}\text{N}$ signal as calculated by the Schwander model which then serves as an input for the firn model from Spahni et al. (2003) to calculate the damping caused by diffusion (dashed line) and additional gradual bubble enclosure (dark blue solid line). According to the model, the signal amplitude between diffusion and bubble enclosure is damped by roughly 30 %. The light blue lines show a $\delta^{15}\text{N}$ signal smoothed by gradual bubble enclosure of a $+7$ and $+13^\circ\text{C}$ temperature increase which corresponds to the uncertainty interval of the temperature amplitude. The grey line shows a $\delta^{15}\text{N}$ signal as calculated by the Schwander model where the input data of a temperature increase ($+10^\circ\text{C}$ in 20 yr) is splined with 200 yr. Diamonds represent $\delta^{15}\text{N}$ measurements for DO 8 from NGRIP (green, uncertainty: $\pm 0.02\text{‰}$, this study) and NEEM (violet, uncertainty: $\pm 0.006\text{‰}$, from Guillevic et al., 2013). The scale on the x-axis is chosen in a way that 0 yr corresponds to the beginning of the surface warming. All data are plotted on a gas age scale. **(b)** Surface (solid line) and LID temperature (dotted line) are given for the $+10^\circ\text{C}$ temperature increase as calculated by the Schwander model.

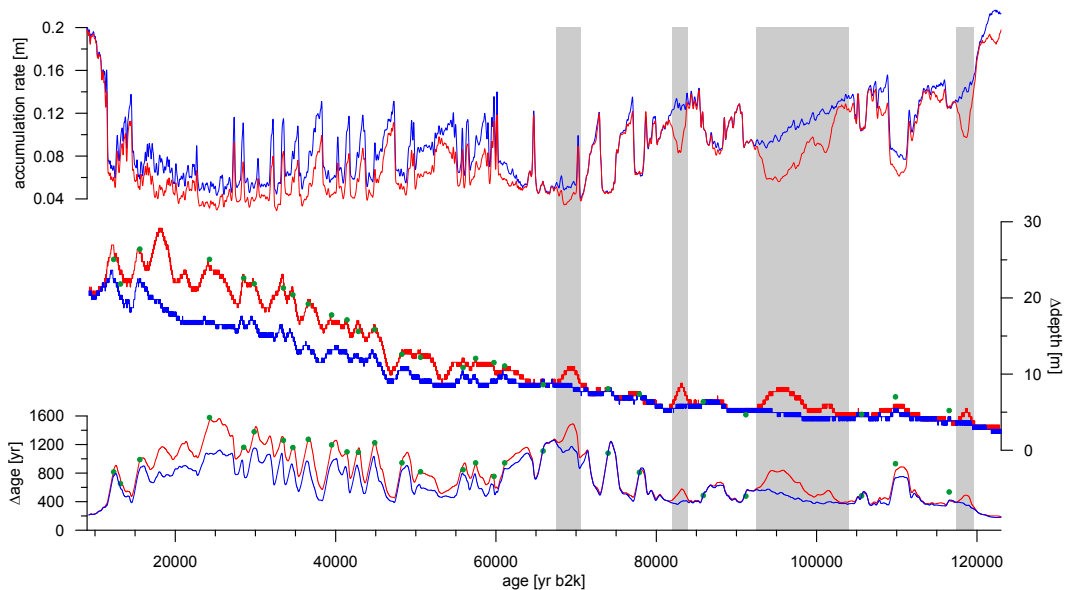


Fig. 4. Top graph: the blue line corresponds to the accumulation rate given by the ss09sea06bm time scale, the red line indicates the reduced accumulation rate which was used for the temperature reconstruction. Middle graph: modelled Δ depth, once with the reduced accumulation rate (red) and once with the original accumulation rate (blue), green points are measurements. Bottom graph: modelled Δ age, once with the reduced accumulation rate (red) and once with the original accumulation rate (blue), green points are Δ age measurements. The grey bars mark periods where the accumulation rate was significantly reduced without a possibility to check this correction by the help of Δ age and Δ depth.

NGRIP temperature reconstruction from 10 to 120 kyr b2k

P. Kindler et al.

[Title Page](#)

[Abstract](#) [Introduction](#)

[Conclusions](#) [References](#)

[Tables](#) [Figures](#)

[⏪](#) [⏩](#)

[◀](#) [▶](#)

[Back](#) [Close](#)

[Full Screen / Esc](#)

[Printer-friendly Version](#)

[Interactive Discussion](#)



NGRIP temperature reconstruction from 10 to 120 kyr b2k

P. Kindler et al.

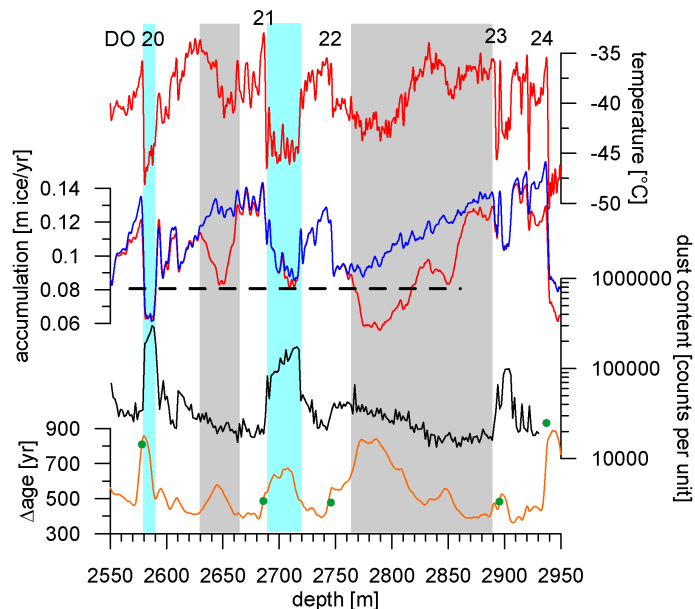


Fig. 5. The top red line shows the temperature transformed to a depth scale, numbers indicate the DO events. Unchanged and reduced accumulation rate are represented by the blue and red line, respectively, the black line shows the dust content (Ruth et al., 2003) and the orange line the Δ age, green dots are Δ age measurements.

Title Page

Abstract

Introduction

Conclusions

References

Tables

Figures

⏪

⏩

◀

▶

Back

Close

Full Screen / Esc

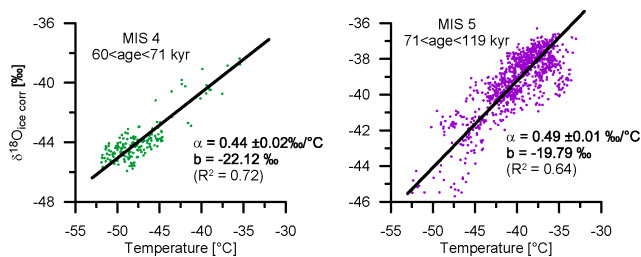
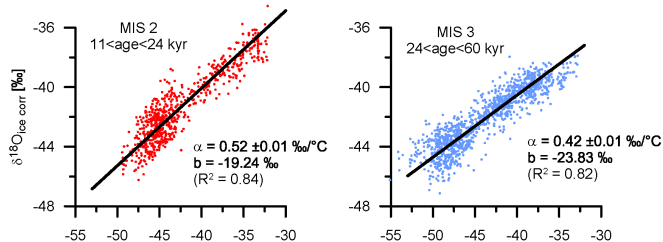
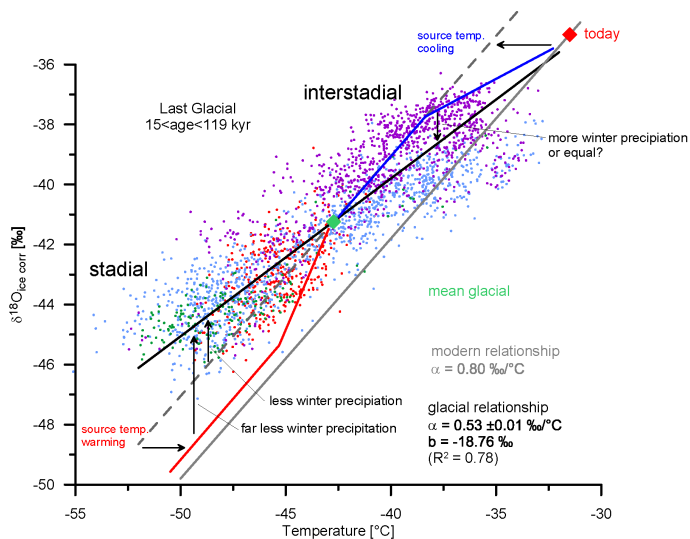
Printer-friendly Version

Interactive Discussion



NGRIP temperature reconstruction from 10 to 120 kyr b2k

P. Kindler et al.



Title Page

Abstract

Introduction

Conclusions

References

Tables

Figures



Back

Close

Full Screen / Esc

Printer-friendly Version

Interactive Discussion



Fig. 6. Relationship of NGRIP $\delta^{18}\text{O}_{\text{ice}}$, corrected for the influence of the glacial isotopic composition of the ocean after Jouzel et al. (2003) and temperature during the whole glacial (upper graph) and during the single MIS separately (four lower graphs). α is the slope of the black regression lines, b the intercept with the ordinate. Same colours are used for different time periods in the upper glacial graph and the four lower graphs. Upper graph: during the interstadials, the expected precipitation isotopy is shifted from the grey (Sjolte et al., 2011) to the blue line because of the source temperature cooling. On the other hand, we suggest that the expected precipitation isotopy should be shifted to lower values during stadials because of the precipitation source temperature warming. The discrepancy between the expected isotopic values (blue and red lines, respectively) and the observed relationship (black line) can be explained by more winter precipitation in interstadials and far less winter precipitation during stadials.

NGRIP temperature reconstruction from 10 to 120 kyr b2k

P. Kindler et al.

[Title Page](#)[Abstract](#)[Introduction](#)[Conclusions](#)[References](#)[Tables](#)[Figures](#)[⏪](#)[⏩](#)[◀](#)[▶](#)[Back](#)[Close](#)[Full Screen / Esc](#)[Printer-friendly Version](#)[Interactive Discussion](#)

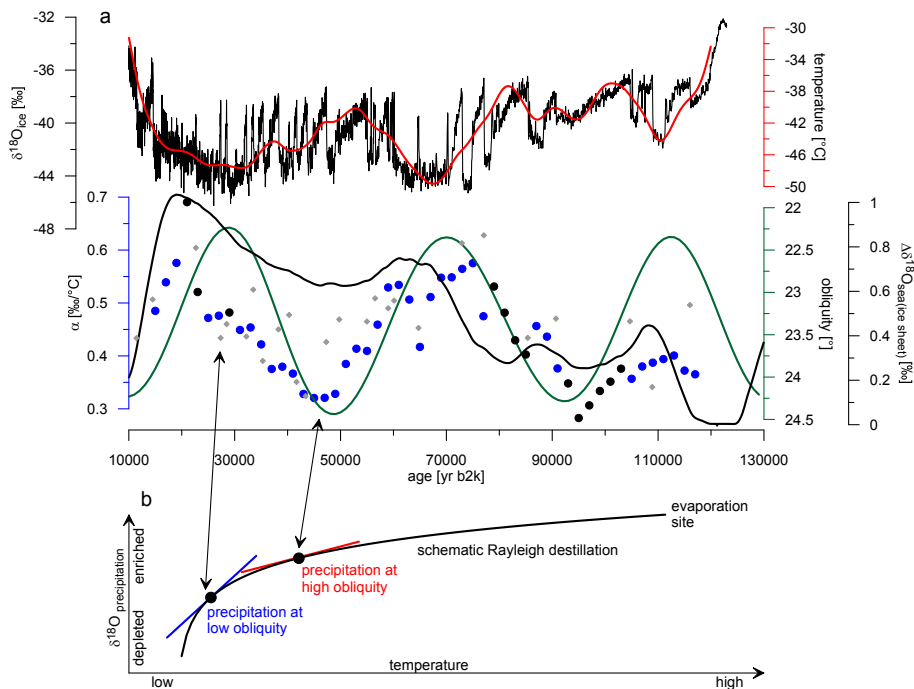


Fig. 7. Comparison between α and obliquity. **(a)** When α is calculated over a time period of 10 kyr (blue points with a R^2 value higher than 0.70, black points with $0.47 < R^2 < 0.70$), a relationship with obliquity (green line, Berger and Loutre, 1991) emerge. No relationship is observed when α is only calculated for single DO events (grey diamonds). While temperature (red line, 10 kyr spline) follows obliquity a lag of α behind obliquity can be observed in the course of the glacial period. $\Delta\delta^{18}\text{O}_{\text{sea}}$, corrected for the influence of the ice sheet volume (Bintanja et al., 2005), as a proxy for the ice sheet extent is shown by the lower black line. **(b)** Schematic Rayleigh model to explain the α variations.